inorganics

MDPI

Review

Recent Developments in the Use of Covalent Organic Frameworks for Photocatalytic Water Decontamination

Víctor Cepa-López [1], Miguel Sánchez-Fuente [1], Alicia Moya [1,*] and Rubén Mas-Ballesté [1,2,*]

[1] Department of Inorganic Chemistry (Module 7), Facultad de Ciencias, Universidad Autónoma de Madrid, 28049 Madrid, Spain; victor.cepa@estudiante.uam.es (V.C.-L.); miguel.sanchezd@uam.es (M.S.-F.)
[2] Institute for Advanced Research in Chemical Sciences (IAdChem), Universidad Autónoma de Madrid, 28049 Madrid, Spain
* Correspondence: alicia.moya@uam.es (A.M.); ruben.mas@uam.es (R.M.-B.)

Abstract: Water pollution by persistent organic and inorganic contaminants constitutes a significant problem for ecosystems and public health. Organic substances such as dyes, pharmaceutical residues, pesticides, and phenolic compounds are increasingly detected in water due to industrial and agricultural activities. Alongside these, toxic heavy metals contribute to the complexity of water treatment challenges. Conventional remediation methods often fall short due to high operational costs or limited efficiency. In this context, photocatalysis has emerged as a promising approach for pollutant degradation in water under light irradiation. In this sense, covalent organic frameworks (COFs), a class of porous, crystalline materials formed by the covalent linkage of organic units, offer great advantages as photocatalysts. Their tunable electronic properties, structural diversity, and high stability under aqueous conditions make them ideal for visible light-driven processes. This review explores the structural features that govern the photocatalytic activity of COFs, including conjugation, bandgap modulation, and donor–acceptor structures. Mechanistic insights into photocatalytic degradation are also discussed. Finally, examples of pre-designed COFs are presented with their application in the photodegradation of water pollutants, and their main reactive oxygen species (ROS) involved in the photodegradation mechanism. Overall, this review aims to provide a foundation for the rational design of COFs in advanced water treatment technologies.

Keywords: covalent organic framework; catalysis; photocatalysis; water decontamination

check for updates

Academic Editor: Francis Verpoort

Received: 8 April 2025
Revised: 28 April 2025
Accepted: 30 April 2025
Published: 6 May 2025

Citation: Cepa-López, V.; Sánchez-Fuente, M.; Moya, A.; Mas-Ballesté, R. Recent Developments in the Use of Covalent Organic Frameworks for Photocatalytic Water Decontamination. *Inorganics* **2025**, *13*, 152. https://doi.org/10.3390/inorganics13050152

Copyright: © 2025 by the authors. Licensee MDPI, Basel, Switzerland. This article is an open access article distributed under the terms and conditions of the Creative Commons Attribution (CC BY) license (https://creativecommons.org/licenses/by/4.0/).

1. Introduction

The limited availability of safe drinking water is a growing problem worldwide [1]. In fact, water is related to many aspects of economic and social challenges and is itself one of the main objectives of sustainable development. In recent decades, several new organic compounds have found their way into water supplies because of intense human activities. Among others, synthetic dyes, pesticides, and pharmaceutical and phenolic compounds have increasingly contaminated water sources [2]. Synthetic dyes, extensively used in the textile, food, and cosmetic industries, are highly stable and their strong coloration can reduce light penetration, affecting aquatic photosynthesis [3,4]. Pharmaceutical compounds, including antibiotics (and analgesics), enter water bodies and, even at trace levels, they can contribute to the development of antibiotic resistance [5]. Additionally, pesticides, widely used in agriculture, can leach into groundwater and surface water, leading to long-term environmental persistence [6]. Phenolic compounds, commonly found in petrochemical

plants, and paper production, are known for their high toxicity and resistance to degradation, which pose a significant threat to aquatic ecosystems and human health [7]. The adverse effects of these pollutants on flora, fauna, and humans can be catastrophic. In addition to their potential toxicity, organic compounds can cause taste and odor problems in water. Unfortunately, once introduced into the environment, some of these compounds are extremely persistent due to their high chemical stability. Apart from organic molecules, a high concentration of heavy metals and other inorganic pollutants contaminate water in industrial environments [8]. In general, these pollutants are not biodegradable, so they can persist largely in the environment. The accumulation of heavy metals is a serious public health problem. For example, Cr(VI) can easily be absorbed by the human body where it acts as a mutagen, carcinogen, and teratogen [9]. The sources of these metals are diverse and are largely related to several industrial applications in chrome plating, dye manufacturing, the textile industry, the aircraft industry, leather tanning, wood preservation, and mud drilling.

Considering the consequences of water pollution, it is obvious that they constitute a global problem in today's interconnected world. Therefore, it is highly desirable to look for integrative approaches that simultaneously address several types of contaminants without the formation of significant toxic by-products. A classic way to decontaminate water is the use of chlorine or ClO_2 for the oxidative degradation of organic and biological matter [10]. In addition, among the conventional processes to remove heavy metals from wastewater, the most used is chemical precipitation, which involves the formation of their insoluble hydroxides, carbonates, or sulfides, followed by sedimentation and filtration [11]. Although effective, these procedures involve costly infrastructures, the use of toxic reagents and the extensive formation of residues. It is therefore necessary to explore alternatives that avoid these drawbacks. For this reason, new strategies have been explored in recent years that take advantage of light energy to trigger photocatalytic processes in the degradation or detoxification of pollutants [12]. Thus, many photooxidative processes are based on the light-induced formation of reactive oxygen species mediated by photosensitizers. These ROS can be radical species, such as hydroxyl anion and/or superoxide, or singlet oxygen, which are effective in the oxidative degradation of organic and biological pollutants. On the other hand, photoreductive transformations, which are usually concomitant to the oxidation of water or additional organic molecules, can also be applied to detoxify heavy metal species.

Although the ability of separating the photosensitizer from solution is crucial in water treatment, heterogeneous systems have been scarcely explored in pollutant photodegradation [13]. A typical approach relied on the use of TiO_2-based materials as a leading photocatalyst due to its low cost, high chemical stability, non-toxicity, and resistance to photocorrosion, but is limited to the use of ultraviolet irradiation [14–16]. In this sense, reticular chemistry, based on linking molecular building blocks by strong bonds to make open frameworks, offers many new possibilities on the discovery of new photoactive systems able to use visible light to trigger predetermined processes. Particularly relevant are covalent organic frameworks, which are based in the atomically precise integration of pure organic units through covalent bonds to create pre-designed skeletons and pores, constituting a main family of reticular porous materials [17]. COFs possesses a highly tunable and predictable pore size and structure, easily tailored functionality, and a versatile covalent combination of building blocks. Because they are composed of light-weight elements linked by strong covalent bonds, they have low mass densities and possess high thermal stabilities [18]. Furthermore, a wide variety of organic building blocks is available with a range of different organic groups that result in well-established condensation reactions.

Therefore, the outstanding properties of COFs make them very attractive and prompted us to investigate their application in the light-mediated decontamination of water.

In recent years, the application of covalent organic structures to photocatalytic processes has experienced a great blossoming [19–22]. As a specific application of this field, the degradation of pollutants has become one of the main focuses of interest, due to its social relevance. Although this area is rapidly reaching considerable maturity, important open questions remain. For example, structure–reactivity relationships in photoactive COFs are currently the subject of debate in the current literature. In this review, we present a critical description of the structural principles affecting the photocatalytic activity of COFs. In particular, conjugation and bandgap tuning of materials, together with donor–acceptor architectures, are reviewed as main strategies to modulate photocatalytic activities. In addition, understanding photocatalytic mechanisms is valuable information needed to rationally design improved photocatalytic systems. Thus, this review presents the current knowledge of the photocatalytic pathways determined for COFs. Finally, numerous examples of the application of COFs to the decontamination of pharmaceutical compounds, organic dyes, pesticides, phenolic compounds, and heavy metal species are summarized in the final part of this manuscript. Considering the large amount of available literature, this review article is not intended to be an exhaustive compilation of published studies. Instead, we have selected the cited literature according to two main criteria: (1) We have given priority to the most recent reports and (2) we have chosen the most representative examples to illustrate the concepts presented in this manuscript. A systematic literature review, such as the one presented in this manuscript, should serve as a guide for future studies devoted to the design of new materials with photocatalytic properties useful for water decontamination.

2. Structure–Activity Relationships

The photocatalytic efficiency of covalent organic frameworks (COFs) for water decontamination is strongly linked to their structural features. Crystal alignment, defect presence, and overall morphology determine their band structure, which, in turn, impacts their photocatalytic performance. These factors influence the modulation of COF optoelectronic properties, ensuring efficient charge and energy transfer processes, both essential for the photodegradation of water pollutants.

COFs are semiconducting materials formed by the valence band (VB), composed of filled atomic orbitals, and the conduction band (CB), formed by empty orbitals. These bands are separated by an energy gap (Eg), containing forbidden energy states. When irradiated with photons of higher energy than the COF bandgap, electrons are excited from the VB to the CB. However, fast electron–hole recombination occurs in most semiconductors, leading to poorer optoelectronic properties and lower photocatalytic activity. Modifying semiconductor structure to trap or extract charge carriers is an established strategy for improving charge separation, and thus photocatalytic efficiency. This review focuses on three key strategies for optimizing COF structures and fine-tuning the COF optoelectronic properties, namely (1) the incorporation of donor–acceptor units into the COF to improve charge separation; (2) the enhancement of π-conjugation across the COF; and (3) modulation of the bandgap energy and COF band positions for improved photocatalysis.

2.1. Donor–Acceptor

Incorporating donor–acceptor (D-A) units into the backbone of photoactive COF is a powerful approach to enhance the photocatalytic degradation of water pollutants. Predesigning COFs containing alternating electron-rich donor and electron-deficient acceptor fragments broadens their optical absorption, while also promoting efficient separation and

transfer of photogenerated electron–hole pairs [23]. This structure significantly reduces recombination, extending electron lifetimes and enabling the generation of reactive oxygen species (ROS), such as hydroxyl radicals and superoxide radical anions, which are critical for oxidizing and degrading organic pollutants in water.

The spatial arrangement of donor and acceptor units within COFs, often incorporating heteroatoms, is a critical factor for efficient charge transfer. For instance, the introduction of benzothiadiazol (acceptor) with halogen substituents and pyrene (donor) units within an imine-based COF has been shown to suppress charge recombination and enhance water splitting (Figure 1a) [24]. Li et al. synthesized an ethylene-linked COF (Py-BSZ-COF) also using pyrene and benzothiadiazole as donor and acceptor fragments (Figure 1b) [25]. This combination resulted in a lower bandgap and faster charge separation, producing superoxide radicals under visible light for catalytic reactions, including oxidative amine coupling and thioamide cyclization to 1,2,4-thidiazole. Furthermore, incorporating benzothiadiazole as a building block extended the light absorption, leading to a red-shift in the absorption edge when compared to equivalent COFs but without this unit.

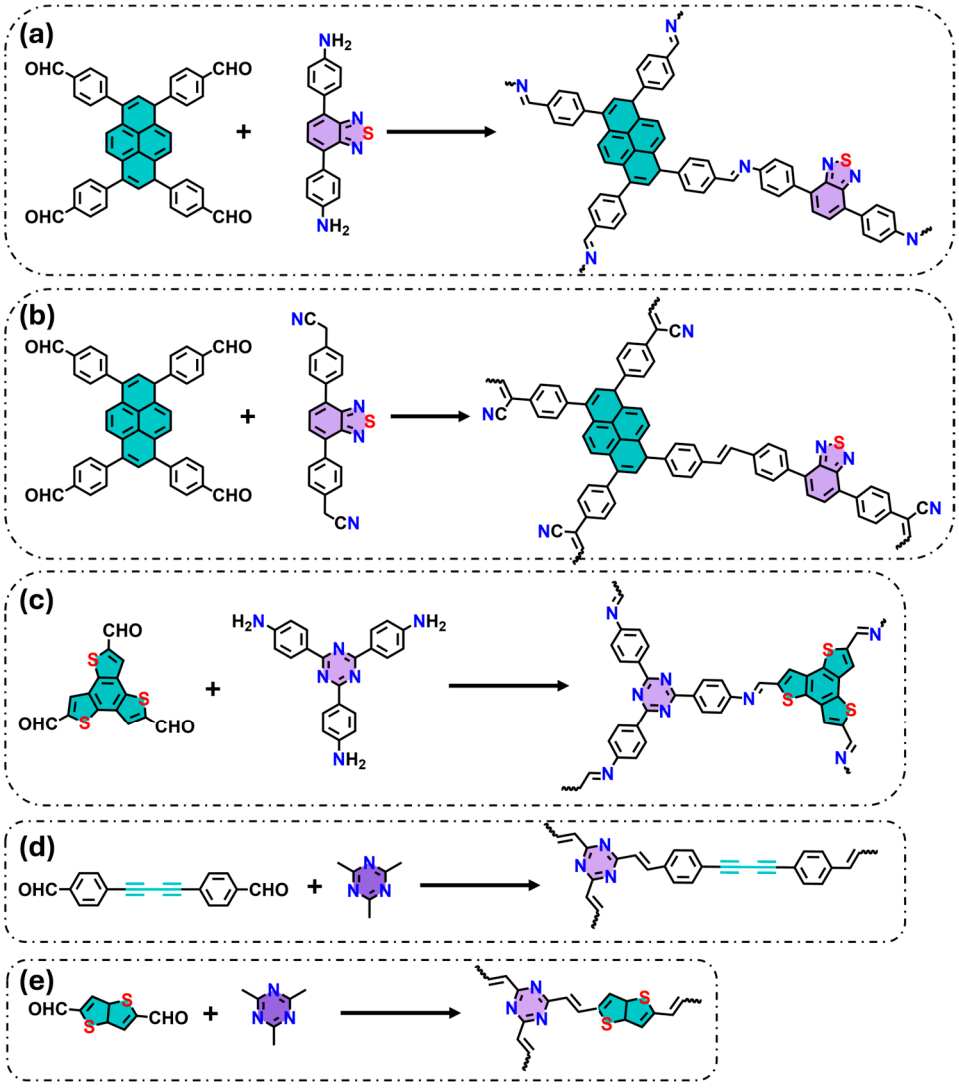


Figure 1. Examples of donor–acceptor precursors used to form new photoactive COFs: (**a**) imine COF formed by pyrene and benzothidiazole, (**b**) vinylene COF formed by pyrene and benzothidiazole, (**c**) imine COF formed by benzotrithiophene and triazine, (**d**) vinylene COF formed by diacetylene and triazine, (**e**) vinylene COF formed by benzotrithiophene and triazine. Green and purple colors indicate donor and acceptor molecules, respectively.

Additionally, triazine-based COFs offer many structural advantages. The triazine moiety with a large number of nitrogen atoms, which act as electron acceptors, improves charge separation and ROS generation. For example, Qing et al. designed imine-linked COFs incorporating triazine (acceptor) and benzotrithiophene (donor), achieving spatially separated donor–acceptor centers (Figure 1c) [26]. This D-A arrangement enhanced electron distribution within the COF and codirectional charge transfer, resulting in high H_2O_2 production. Similarly, Chen et al. designed vinylene-linked COFs combining triazine (acceptor) and diacetylene (donor) derivatives (Figure 1d), and demonstrated impressive photocatalytic degradation of phenol and norfloxacin by more than 96% in 15 min [27]. Deng et al. reported vinylene-linked COFs (TMT-TT-COF) with triazine and heteroatom-rich donor molecules (thieno [3,2-b]thiophene-2,5dicarboxaldehyde), creating narrow bandgaps and efficient charge transport (low recombination rates), resulting in high performance for photocatalytic H_2O_2 production and bisphenol A (BPA) degradation (Figure 1e) [28].

In summary, the donor–acceptor design in COF promotes long-range charge transport to targeted pollutants or oxygen molecules for generating ROS, key agents for the degradation of organic pollutants.

2.2. Conjugation Tunning

Increasing the degree of π-conjugation within COFs is another strategy to improve photocatalytic performance. Extensive π-conjugation in COFs allows better light absorption and faster charge transport, thereby enhancing charge transfer (from light-absorbing regions to reactive sites) while reducing recombination. Higher conjugation facilitates the delocalization of electrons across the COF, optimizing its electronic properties for photocatalysis.

The ability to fine-tune the degree of conjugation in COFs enables optimization for specific light sources and pollutant targets. Lin et al. synthesized two hydrazone-linked COFs with biphenyl (BPh−COF) or acetylene (AC−COF) to evaluate the effect of conjugation on photocatalytic efficiency (Figure 2) [29]. The biphenyl ligands in the BPh−COF offer rigidity and strong conjugation. However, the ethynyl skeleton in the AC-COF enhances planarity and improves the π-conjugation. This significantly improved the optoelectronic properties of AC-COF compared with BPh-COF by narrowing the bandgap energy and improving charge transfer, ultimately enhancing photocatalytic efficiency for oxidative coupling amines. Furthermore, fully conjugated carbon–carbon double bonds in vinylene-linked COFs' prevent spatial distortions, leading to a more efficient conjugated structure.

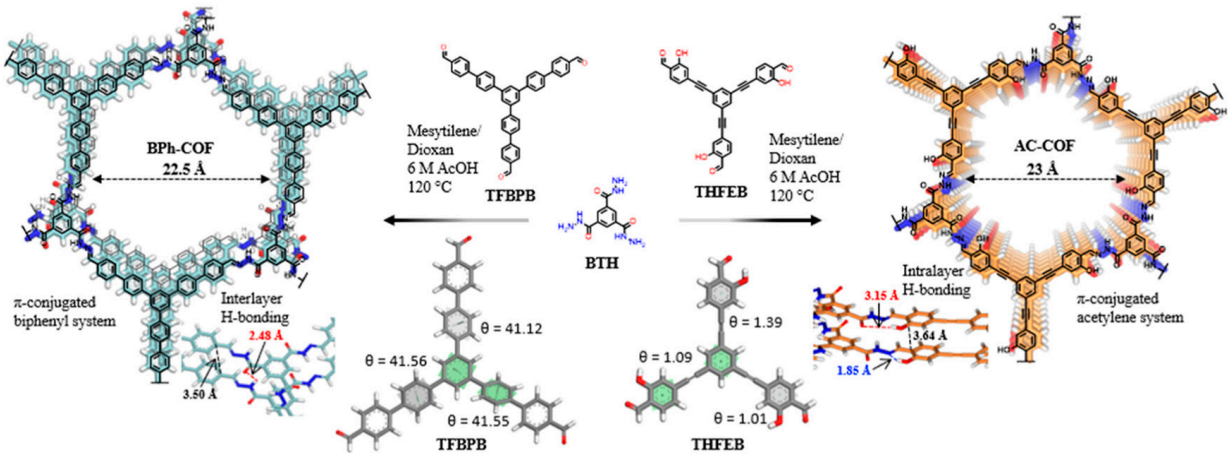


Figure 2. Example of extended π-conjugated COFs (adapted with permission from [29]).

Additionally, Deng et al. presented a post-synthetic modification of imine COFs by sulfurization, leading to thiazole-linked frameworks with enhanced π-conjugation [30]. The

resulting sulfurized COFs exhibited superior charge transport, increasing the photocatalytic H_2O_2 production when applied in oxygen reduction reactions (ORRs) by nearly six times more than pristine COF. This work highlights the importance of conjugation tunning and details a post-synthetic sulfurization for improving the local conjugation of imine-linked COFs and therefore, their photocatalytic activity.

2.3. Bandgap Modulation and Band Positioning for Optimal Photocatalysis

Modulating the COF bandgap and positioning the VB and CB are key strategies for optimizing electron transfer and maximizing photocatalytic efficiency. A narrower bandgap allows COFs to absorb more visible light, making them ideal for sunlight-driven photocatalysis in water remediation. Additionally, aligning VB and CB of the COFs with the redox potentials of pollutants creates more effective electron-holes, increasing photocatalytic degradation rates.

Chen et al. synthesized a family of hydrazide-based COFs modulating its band structure by incorporating different linkers [31]. They demonstrated improved bandgap tunning and charge transfer through intersystem crossing (ISC) from the S_1 excited state to the triplet state (T_1) under visible light. This boosted remarkable photocatalytic performance in applications like uranium extraction from water sources. However, it is well known that the photocatalytic efficiency of single-component catalysts is limited by the photocarrier recombination [32]. COF-based heterojunction has been reported as an alternative for improving band-bending. When COFs are combined with other semiconductors and form a heterojunction, band-bending occurs depending on the type of majority charge carriers (electrons or holes). In the literature, X-ray and Ultraviolet Photoelectron Spectroscopy (XPS and UPS) has been employed to determine Fermi level (E_F, energy level with the 50% probability of being occupied by an electron) position of different photocatalysts, which enables researchers to predict their band-bending [33,34]. Furthermore, band-bending also occurs when a semiconductor is in contact with a wastewater solution. Electrons will flow until the Fermi level of the solid is equalized with the redox potential of the pollutant (E_{redox}), and the energy barrier formed on the solid–liquid interface is denoted as flat band potential (V_{fb}). This parameter can be experimentally estimated from electrochemical characterization by measuring the capacity of the semiconductor–electrolyte interface as a function of applied potential, known as a Mott–Schottky plot.

Many examples of engineering band-bending in COFs have been reported to enhance charge carrier lifetime and interaction with pollutants, ensuring more efficient photocatalytic degradation. For example, covalent bonding between COFs and MOF has appeared as a promising research direction to enhance the degradation of organic pollutants. For instance, He et al. prepared a COF/MOF composite (NH_2-MIL-125 (Ti)/TTB-TTA) and, based on the valence band XPS spectra, they estimated the energy position of the VB and CB of the composite materials and the individual counterparts [35]. Yang et al. also adopt this strategy and combine Ti-MOF and COF with triazine moieties (Figure 3a) [36]. Furthermore, they used photocurrent and electrochemical impedance spectroscopy (EIS) measurements and demonstrated an effective charge transfer in the heterojunction. This hindered recombination and enabled an efficient photocatalytic degradation of bisphenol A.

Other examples of COF-based heterojunctions are their combination with well-known inorganic photocatalysts, solving the disadvantages of wide bandgap and the high electron–hole recombination rate of the inorganic semiconductors. For example, Liu et al. prepared Fe–TiO_2@COF with exceptional photodegradation efficiency for methylene blue [37]. Furthermore, Liu et al. synthesized a COF-PD/AgI composite which showed excellent degradation of rhodamine B and acetaminophen (Figure 3b) [38]. Sun et al. constructed a CdS/COF composite for the photodegradation of bisphenol A (BPA) [39]. More sophisticated sys-

tems were reported by the immobilization of electron mediator ($[Cp^*Rh(bpy)H_2O]^{2+}$) on COFs supported on silica matrix (Figure 3c) [40]. In addition, the combination of COFs with visible light-responsive semiconductor photocatalyst graphite carbonitride (g-C_3N_4) has recently attracted great attention in the photocatalytic degradation of pollutants (Figure 3d). For instance, the heterojunction formed in composites g-C_3N_4@COF has been proven effective in enhancing charge mobility and reducing electron–hole recombination rates [41–43]. These composites exhibit high photocatalytic efficiency toward the degradation of organic pollutants due to the optimal balance between the nitrogen content and graphitization degree.

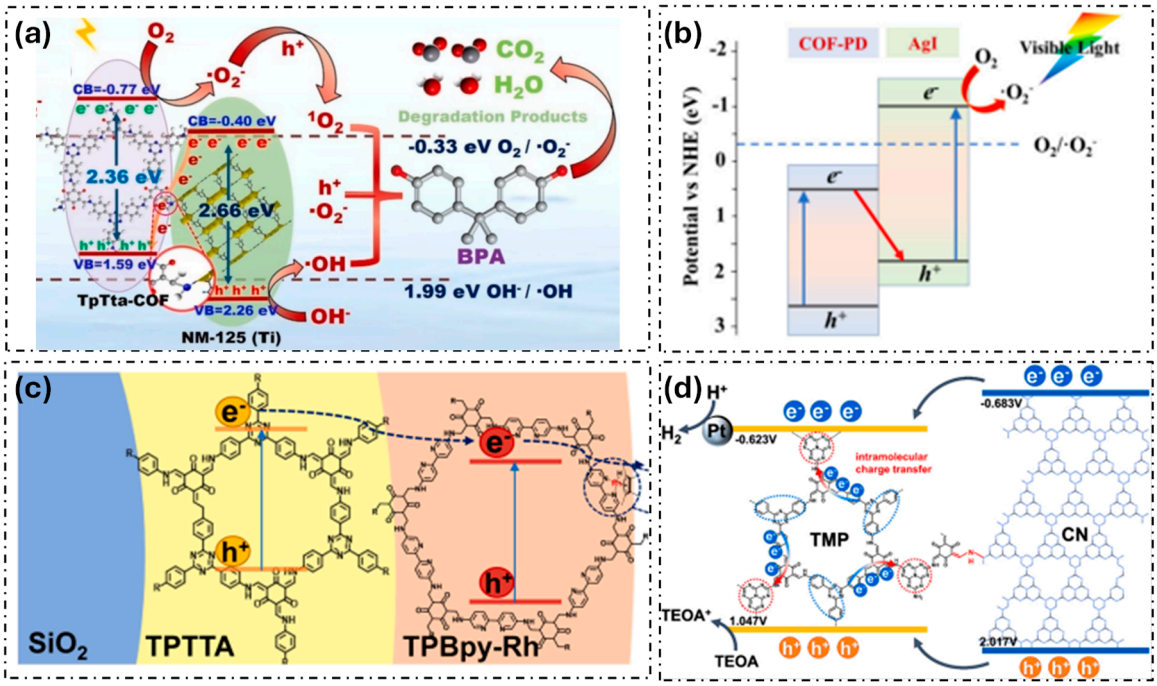


Figure 3. Examples of COF-based heterojunctions used as photocatalytic systems: (**a**) TpTta-COF/NM-125(Ti) (adapted with permission from [36]), (**b**) COF-PD/AgI (adapted with permission from [38]), (**c**) ($[Cp^*Rh(bpy)H_2O]^{2+}$)/COFs (adapted with permission from [40]), and (**d**) g-C_3N_4@COF (adapted with permission from [43]).

2.4. Synergistic Strategies

COFs present a highly tunable structural platform for enhancing photocatalytic water decontamination. Structural modifications, particularly donor–acceptor integration, π-conjugation tuning, and modulation of bandgap and band position, are key strategies for improving photocatalytic performance. However, the combined or synergistic implementation of these approaches can yield higher photocatalytic activities than individual strategies alone. For example, the presence of donor–acceptor motifs in an extended π-conjugated COF can simultaneously maximize light absorption, enhance charge separation, and facilitate charge transport [30,44,45]. Similarly, these pre-designed COFs with inherent D–A character and high conjugation can be combined with other materials, leading to heterojunctions able to extend the photocarrier lifetime and decrease bandgap energy towards visible range, ultimately reinforcing the photocatalytic efficiency of the system [46,47].

Overall, the rational design of COFs through synergistic strategies will be pivotal for optimizing photocatalytic materials for water decontamination. The structure–property relationships must be optimized to increase the potential of COFs in green and sustainable water purification technologies. This knowledge will be critical to establishing the best

COF structures for degrading specific water pollutants with ongoing advancements in COF synthesis and functionalization. Their potential for environmental remediation is expected to expand, offering green solutions for degrading persistent water pollutants.

3. General Photocatalytic Mechanisms

Photocatalysis generally implies the absorption of a photon by a photocatalyst, leading to its excited electronic state. In this process, the photon energy (hυ) must be equal to or greater than the energy gap between the valence and conduction bands (or the HOMO-LUMO gap in the case of molecular photocatalysts). Upon absorption, an electron is excited from the lowest occupied energy level to a higher energy state in the conduction band, increasing its reactivity [48]. The excited photocatalyst can return to its ground state through two primary mechanisms: Single Electron Transfer (SET) and energy transfer (EnT). In SET, an electron exchange occurs between the photocatalyst in its excited state and a substrate (such as a pollutant) or a cocatalyst within the reaction system [49]. In contrast, EnT involves the transfer of the absorbed photon energy from the photoexcited catalyst to a substrate or cocatalyst in a radiative or non-radiative way, inducing a chemical transformation [50]. Once this process concludes, the excited electron returns to the ground state (Figure 4).

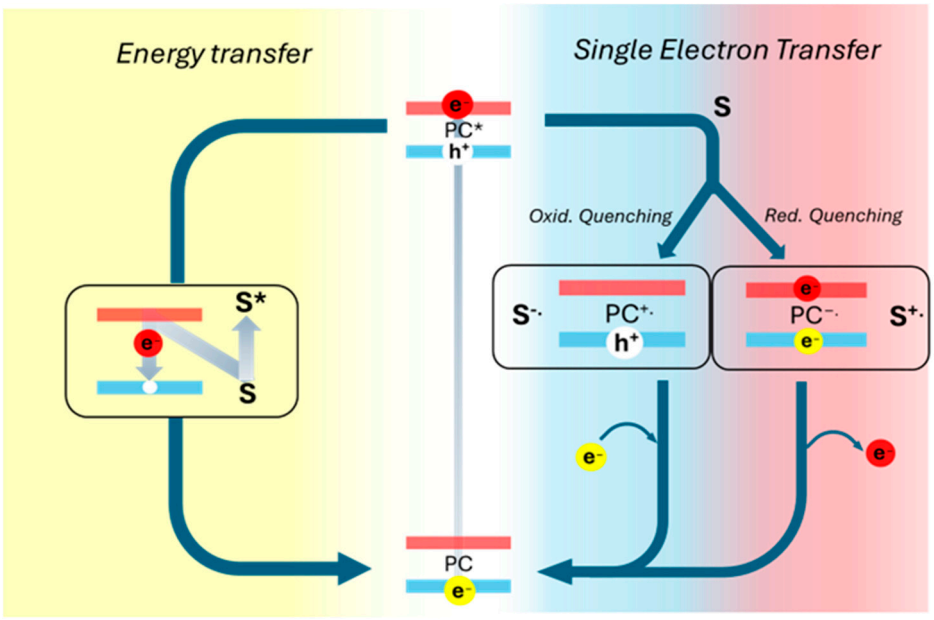


Figure 4. Schematic representation of energy transfer processes and singlet electron transfer process. (*) indicates the excited electronic state of the photocatalyst (PC).

3.1. Electron Transfer: Reductive Quenching vs. Oxidative Quenching

Electron transfer between the photocatalyst and a substrate (pollutant) or cocatalyst can proceed via two distinct pathways, depending on the redox potentials and the relative energy levels of the conduction and valence bands of the photocatalyst compared to the HOMO-LUMO levels of the substrate [51].

On the one hand, if the reduction potential of the photocatalyst is higher than that of the substrate ($E^{S}_{red} < E^{PC}_{red}$), oxidative quenching occurs. This process is favored when the conduction band of the photocatalyst is energetically higher than the LUMO of the substrate. Oxidative quenching results in substrate reduction, generating a radical anion ($S^{-\cdot}$) and a radical cation of the photocatalyst ($PC^{+\cdot}$). The radical cation is subsequently reduced by a regenerator (R), closing the catalytic cycle. This regenerator may be a Sacrificial Electron Donor (SED), or another compound involved in the mechanism (Figure 5). On the other

hand, if the reduction potential of the substrate is higher than that of the photocatalyst ($E^{PC}_{red} < E^{S}_{red}$), reductive quenching is favored. In this case, electron transfer occurs from the substrate to the photocatalyst, generating an oxidized substrate intermediate ($S^{+\cdot}$) and a radical anion of the photocatalyst ($PC^{-\cdot}$). The radical anion then transfers its extra electron to the regenerator, completing the catalytic cycle (Figure 5).

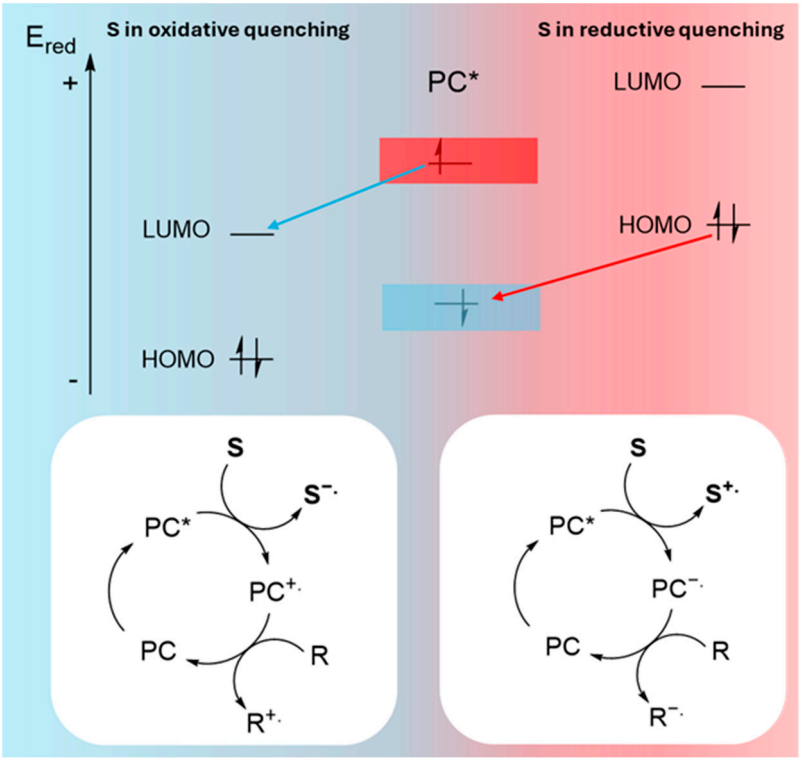


Figure 5. Schematic representation of oxidative and reductive quenching. (*) indicates the excited electronic state of the photocatalyst (PC).

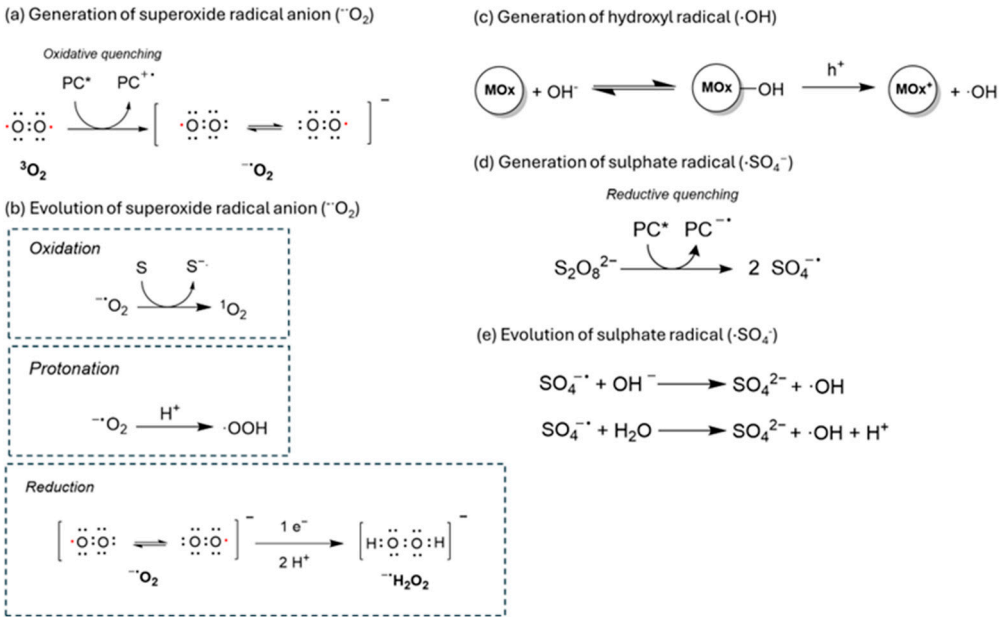
These electron transfer pathways are very common in various photocatalytic transformations, where radical species act as key intermediates. The reactivity of these species depends on their lifetimes, while their selectivity is influenced by the reactive oxygen species (ROS) involved. Herein, we describe some of the most frequent radical species involved in photocatalytic transformations.

3.2. Generation of Radical Species: Superoxide, Hydroxyl, and Organic Radicals

Radical species are compounds characterized by an unpaired electron. They commonly arise from homolytic cleavage of a covalent bond or through SET-mediated oxidative or reductive quenching mechanisms involving the photocatalyst. These species generally exhibit high reactivity due to their inherent instability. In this section, we will review some of the most frequent radicals involved in photocatalytic oxidation processes related to organic photoactive materials.

Superoxide radical anion ($\cdot O_2^-$) is formed through the oxidative quenching of molecular oxygen with the excited state of a photocatalyst. This radical results from electron transfer from the CB of the photocatalyst to the antibonding π orbital of triplet oxygen. Superoxide radicals are relatively stable due to their extended lifetime. The nature of this radical anion is predominantly oxidative (E_{red} ($\cdot O_2^-/H_2O_2$) = 0.93 V) but can also act as a reductant, presenting in a protic medium and E_{ox} ($O_2/\cdot O_2^-$) = 0.33 V [52]. In fact, these radicals play a crucial role in photocatalytic oxidative couplings and pollutant degradation. For example, the oxidative role of superoxide radical anion is commonly observed

in photocatalytic oxidation of benzylic amines to form amine radical cations in oxidative couplings of amines [53] or in the photocatalytic aerobic degradation of pollutants such as of methylene blue or rhodamine B dyes [54]. Additionally, a superoxide radical anion can be further oxidized to form singlet oxygen, or protonated (see Scheme 1) to form peroxyl radical (·OOH) [55,56].



Scheme 1. A scheme of the evolution of superoxide radical anion to form other oxidant radical species.

Hydroxyl radical(·OH) is a highly oxidant radical species generated by the reduction of hydrogen peroxide via Fenton-type reactions or by the oxidation of hydroxyl anions. These species are commonly observed in metal oxide-based photocatalysis such as TiO_2 [57–59]. However, only a few examples exist of COF materials with metal centers able to produce these hydroxyl radicals. In this sense, some composites with metal like Pd or Ni have been reported in oxidations promoted by hydroxyl radicals [60,61].

The scarcity of examples of pure organic materials able to generate hydroxyl radical could probably be attributed to their lower charge mobility compared with metal-based photocatalysts, which restrict the diffusion of charge carriers to active adsorption sites on the material surface. Consequently, the homolytic cleavage of the O-H bond in water, hydrogen peroxide, and hydroxyl anion species is impaired.

Sulfate radical species (·SO_4^-) have also been reported to be formed from the photocatalytic activation of persulfate ($S_2O_8^{2-}$) anions via reductive quenching with the photocatalyst [62,63]. These species present longer lifetimes than hydroxyl radicals, and in many cases, an enhanced reactivity towards the degradation of different organic molecules. For this reason, they have been reported frequently in the literature in photodegradation mechanisms of pollutants in water [64,65]. Furthermore, sulfate radicals can undergo different transformations in presence of water or hydroxyl groups to promote the formation of ROS (·O_2^-, $^1O_2$ or ·OH).

3.3. Energy Transfer: Singlet Oxygen and Direct Energy Transfer

Chemical transformations can also be promoted through direct energy transfer from the photocatalyst to the substrate, primarily via two different mechanisms, depending the type of excited state reached (Figure 6). In general, after the absorption of a photon, the photocatalyst reaches a primary excited state from which a slight energy decay attributed

to vibrations and thermic loss of energy takes place. This process drives the PC* to a singlet excited state, which can further evolve to a triplet excited state through intersystem crossing (ISC). Depending on the population of either singlet or triplet excited states, we can consider Förster resonance energy transfer (FRET) and Dexter energy transfer mechanisms.

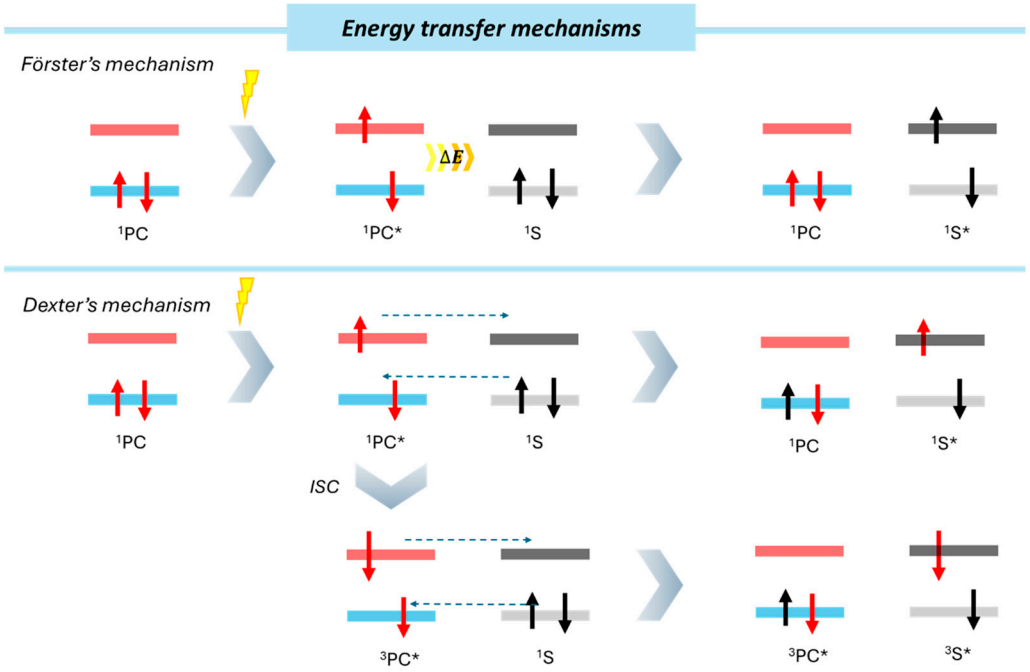


Figure 6. Schematic representation of energy transfer mechanisms. (*) indicates the excited electronic state of the photocatalyst (PC).

Förster's mechanism implies long-range dipole–dipole (Coulombic) interactions from the excited photocatalyst to the substrate. The efficiency of this energy transfer depends on the relative geometric orientation and distance between interacting species. Since heterogeneous photocatalysis occurs at the catalyst's surface, proximity between the substrate and the catalyst active sites is crucial. Different parameters altering the substrate interaction with the photocatalyst, like non-covalent interactions, would have significant influences on the substrate adsorption and would impact energy transfer efficiency.

The Dexter mechanism relies on a short-range electron exchange between the excited photocatalyst and the substrate. Unlike SET, Dexter energy transfer mechanism does not produce charged intermediates and maintains a charge neutrality. This phenomenon requires orbital overlap between the donor (photocatalyst) and the acceptor (substrate), involving collisional interactions. For the viability of this mechanism, short distances (order of Angstroms) are required. In the case of a heterogeneous photocatalyst, an overlap between the "acceptor" substrate orbital and the "donor" band of the material would be required for an efficient energy transfer.

Finally, a well-known example of energy transfer activations is the conversion of triplet oxygen ($^3O_2$) into singlet oxygen ($^1O_2$), a highly reactive oxidant. This transformation has been widely used in photocatalyzed oxidation reactions involving heterogeneous photocatalysts [66–68]. However, the promotion of oxygen from its triplet to singlet excited state is not always favored. Efficient singlet oxygen generation depends on the photocatalyst's ability to undergo intersystem crossing (ISC) to a triplet state. If rapid fluorescence deactivation from the photocatalyst's singlet excited state occurs, the energy transfer process for singlet oxygen formation may be inefficient. Thus, photocatalysts with

extended exciton lifetimes are more suitable candidates for singlet oxygen generation via energy transfer [69].

4. Pollutants Tackled

Covalent organic frameworks offer a promising solution for water decontamination through the photocatalytic degradation of major pollutants, including pharmaceutical compounds, organic dyes, toxic metals, pesticides, and phenolic compounds. Table 1 summarizes various COF-based photocatalysts capable of degrading common pharmaceutical contaminants such as the analgesic acetaminophen and three antibiotics: tetracycline, sulfamethazine, and sulfamethoxazole (Figure 7).

Table 1. COF-based photocatalysts for degradation of pharmaceutical compounds in water.

Pollutant	COF Name (Linkage Type)	Design Principle	ROS Involved	Ref.
Tetracycline	COF-R (imine)	Donor–acceptor COFs	$\cdot O_2^-$/·OH	[70]
	sp^2c-COF (olefin)	Extended conjugation of COFs	·OH	[71]
	MoS_2/COF (imine)	MoS_2/COF heterojunction	·OH/$\cdot O_2^-$	[72]
Acetaminophen	COF-TD1 (imine)	Donor–acceptor COFs	$\cdot O_2^-$	[73]
	COF-PD/AgI (imine)	COF/AgI heterojunction	$\cdot O_2^-$	[38]
	Heptazine-COF@TiO_2 (imine)	COF/TiO_2 heterojunction	$\cdot O_2^-$	[74]
Sulfamethazine	SQ-COF-1 (imine)	Extended conjugation of COFs	$\cdot O_2^-$	[75]
	COF/CN-3 (C-N bond)	COF/g-C_3N_4 heterojunction	$\cdot O_2^-$/$^1O_2$/·OH/$SO_4^{-\cdot}$	[76]
Sulfamethoxazole	COF-909(Cu) (imine)	COF(Cu)	$\cdot O_2^-$/·OH	[77]

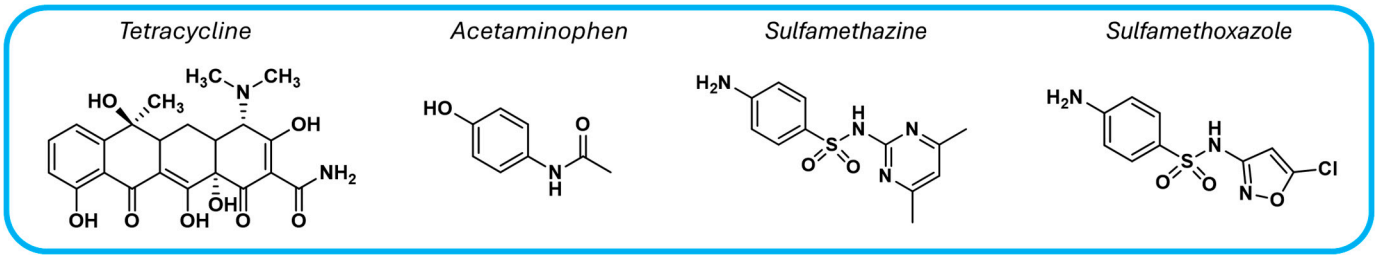


Figure 7. Chemical structures of pharmaceutical compounds commonly found as water pollutants.

Tetracycline (TC) photodegradation has been explored through various synthetic strategies, including donor–acceptor COFs, extended π-conjugated COFs, and inorganic/COF heterojunctions. One approach involves imine-linked COF (COF-R) functionalized with electron-withdrawing (-OH and -OMe) and electron-donating (-Cl, -Br) substituents (Figure 8a). Mechanistic studies indicated that TC degradation primarily occurs through direct oxidation by photogenerated holes, with ROS, particularly $\cdot O_2^-$ and ·OH, also contributing to the TC photodegradation process. The electron-withdrawing groups favor direct oxidation by lowering the valence band energy, whereas electron-donating groups enhances ROS generation [70].

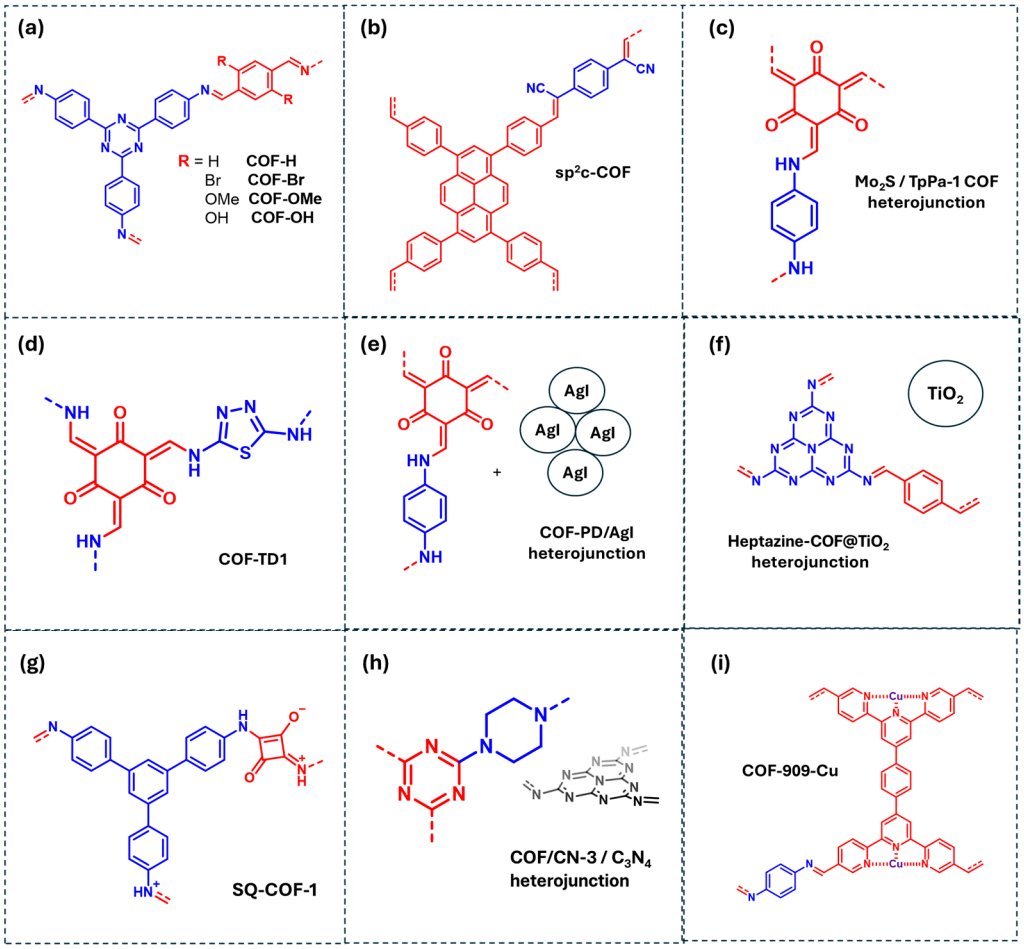


Figure 8. COF-based materials employed as photocatalysts for the degradation of pharmaceutics in water: (**a**) COF-R, (**b**) sp^2c-COF, (**c**) Mo_2S/TpPa-1 COF heterojunction, (**d**) COF-TD1, (**e**) COF-PD/AgI heterojunction, (**f**) Heptazine-COF@TiO_2 heterojunction, (**g**) SQ-COF-1, (**h**) COF/CN-3/C_3N_4 heterojunction, (**i**) COF-909-Cu. Red and blue coloration indicates the two building block units employed for the COF formation.

Another strategy involves the development of olefin-linked COFs with extended π-conjugation, such as sp^2c-COF, which facilitates the delocalization of photogenerated electrons and promotes TC direct oxidation by holes (Figure 8b) [71]. Electron paramagnetic resonance (EPR) analysis confirms the generation of both ·OH and $\cdot O_2^-$, although scavenger studies indicate that only ·OH plays a significant role in TC photodegradation. Additionally, semiconductor/COF heterojunctions, such as MoS_2/COF, have been employed for TC photodegradation (Figure 8c) [72]. In this system, photogenerated electrons in the COF conduction band (CB) transfer to the MoS_2 CB, while holes oxidize TC directly. The electrons in MoS_2 react with molecular O_2 to generate $\cdot O_2^-$, which subsequently forms ·OH via interaction with H_2O, enhancing photocatalytic performance.

For acetaminophen (ACTP) degradation, donor–acceptor COFs have been designed using thiadiazole (donor) and quinone (acceptor) fragments, as COF-TD1 (Figure 8d) [73]. These fragments facilitate charge separation by localizing photogenerated electrons at the acceptor centers and holes at the donor centers, reducing recombination. Mechanistic studies reveal that while direct oxidation by holes is possible, $\cdot O_2^-$ is the primary oxidant species. COF-based heterojunctions have also been investigated for ACTP photodegradation. For example, Liu et al. developed a COF-PD/AgI heterojunction that primary generates $\cdot O_2^-$, which oxidize the acetaminophen molecules (Figure 8e) [38]. Though hydroxyl radicals were detected by EPR, they are inactive in ACTP degradation but contribute

to other photocatalytic processes such as bacteria degradation. Direct oxidation by holes was negligible. Similarly, Ge et al. reported a Heptazine-COF@TiO_2 heterojunction for photocatalytic degradation of dyes and pharmaceuticals (Figure 8f) [74]. Under visible light irradiation, photogenerated electrons in the COF generate $\cdot O_2^-$ or are transferred to the TiO_2 CB, further producing $\cdot O_2^-$, which plays a crucial role in ACTP degradation.

Photodegradation of other antibiotics, such as sulfamethazine (SMT) and sulfamethoxazole (SMX), have also been included in Table 1. Ben et al. synthesized extended π-conjugated COFs via imine condensation of squaric acid (SQ) with 1,3,5-tris(4-aminophenyl)benzene (TAPB), forming SQ-COF-1 (Figure 8g) [75]. The SQ center possesses a more negative charge density than the TAPB fragment, which is mainly positive. Upon illumination, photogenerated electrons localize on SQ, while holes remain on TAPB fragments, increasing their lifetime. Scavenger studies indicate that SMT photodegradation proceeds through $\cdot O_2^-$ oxidation. Furthermore, Qi et al. studied SMT degradation using a COF-based hybrid material, combining PC-COF with g-C_3N_4, forming the COF/CN-3 photocatalyst (Figure 8h) [76]. Under irradiation, COF CB electrons react with molecular O_2 to generate $\cdot O_2^-$, which further evolves into $^1O_2$, both serving as primary reactive species in SMT photodegradation. Additionally, $SO_4^{-\cdot}$ and ·OH radicals were identified as photocatalytic intermediates. Finally, for sulfamethoxazole (SMX) degradation, Table 1 includes a N-rich COF coordinated with Cu, designated COF-909(Cu) (Figure 8i) [77]. Cu coordination with COF nitrogen atoms reduces the bandgap energy and shifts the energy band positions, enhancing photocatalytic performance. Mechanistic studies employing EPR detected ·OH and $\cdot O_2^-$ species. However, a scavenger study is lacking to determine the relative significance of these ROS in SMX degradation.

These studies highlight the versatility of COFs in photocatalytic water decontamination, demonstrating their efficiency in degrading pharmaceutical pollutants through various photocatalytic mechanisms, including direct oxidation and ROS-mediated degradation.

Another important group of toxic substances commonly found in water is the heavy metals, such as uranium U(VI) and chromium Cr(VI), which can be reduced to their non-toxic or less toxic forms, U(IV) and Cr(III), respectively, using COF-based materials (Table 2). In the case of uranium degradation, Zhong et al. reported a β-keto-enamine COFs (TpTt-COF) rich in heteroatoms and containing two electron-acceptor fragments (triazine and ketones) in close proximity (Figure 9a) [78]. These structural features enhance planarity and extend π-conjugation of the COFs, improving the efficiency of photocarrier separation and boosting photocatalytic activity. This COF generates $\cdot O_2^-$ and $^1O_2$ radicals, where $\cdot O_2^-$ actively reduces U(VI) to insoluble U(IV) species such as UO_2, $UO_{2.9}$, $UO_{2.87}$ and $UO_{2.82}$. However, $^1O_2$ can promote the reoxidation of U(IV) to U(VI), which should be minimized by adding scavengers of $^1O_2$.

Table 2. COF-based photocatalysts for reduction of U(VI) and Cr(VI) in water.

Pollutant	COF Name (Linkage Type)	Design Principle	ROS Involved	Ref.
U(VI)	TpTt-COF (imine)	Donor–acceptor COFs	$\cdot O_2^-$	[78]
	DQTP-COF (imine)	Donor–acceptor COFs	$\cdot O_2^-$	[79]
	COF-AQ (imine)	Donor–acceptor COFs	-	[80]
	COF-4-Pd-AO (imine)	COF/Pd heterojunction	-	[81]
Cr(VI)	COFs-OMe (imine)	Donor–acceptor COFs	$\cdot O_2^-$	[70]
	TPB-BT-COF (imine)	Donor–acceptor COFs	-	[82]
	HDU-26-COF (imine)	Donor–acceptor COFs	$\cdot O_2^-$	[83]
	TAPP-2F-COF (imine)	Halogenated COFs	$\cdot O_2^-$	[84]

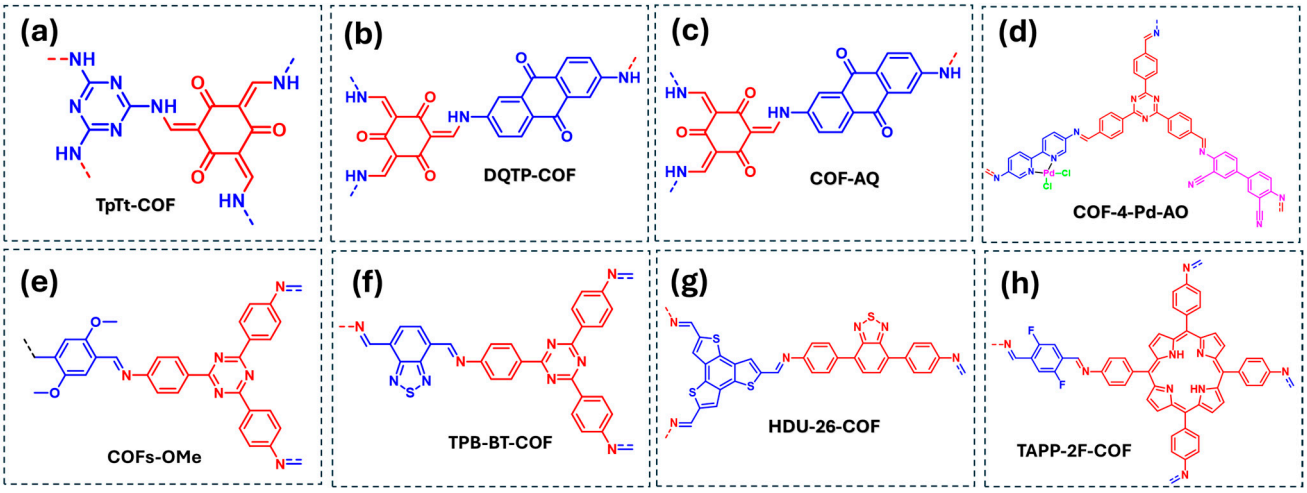


Figure 9. COF-based materials employed as photocatalysts for the reduction of U(VI) and Cr(VI) in water: (**a**) TpTt-COF, (**b**) DQTP-COF, (**c**) COF-AQ, (**d**) COF-4-Pd-AO, (**e**) COFs-OMe, (**f**) TPB-BT-COF, (**g**) HDU-26-COF, (**h**) TAPP-2F-COF. Red and blue coloration indicates the two building block units employed for the COF formation.

Furthermore, Ling et al. presented a COF containing anthraquinone units, which play a crucial role in charge separation and serve as active sites for U(VI) reduction (Figure 9b) [79]. Experimental results identified $\cdot O_2^-$ as the dominant reactive species, while direct electron transfer also contributed to the U(VI) reduction process. The same COF material was further studied for various photocatalytic processes by Huang et al. who designated it as COF-AQ (Figure 9c) [80]. In this study, EPR spectroscopy confirmed the generation of ROS, and scavenger experiments using silver nitrate as an electron quencher demonstrated that the primary photocatalytic reduction mechanism for U(VI) using the COF-AQ involved direct electron transfer. Additionally, Hao et al. designed a COF by incorporating two amine precursors with bipyridine and diciano-biphenyl moieties and 4,4′,4″-(1,3,5-triazine-2,4,6-triyl)tribenzaldehyde (TATTA) [81]. The resulting COF was subsequently functionalized with $PdCl_2$ to produce COF-4-Pd-AO, where Pd centers coordinated to bipyridine units act as active sites for adsorption and photocatalytic uranium reduction (Figure 9d). Mechanistic studies of this COF/Pd heterojunctions concluded that U(VI) species undergo direct electron transfer reduction to UO_2.

Regarding the photoreduction of Cr(VI) species, Zhang et al. investigated the effect of electron-withdrawing and electron-donating substituents in COFs, revealing that methoxy-functionalized COFs (COFs-OMe) exhibit the highest photocatalytic efficiency for Cr(VI) reduction (Figure 9e) [70]. Mechanistic studies demonstrated that Cr(VI) photoreduction occurs through both direct electron transfer and $\cdot O_2^-$ generation, which actively participates in the reduction process. Furthermore, Chen et al. reported a benzodithiazole-containing COF (TPB-BT-COF) with exceptional Cr(VI) photoreduction to Cr(III) species, achieving over 99% efficiency without the need for sacrificial agents or pH adjustment (Figure 9f) [82]. Additionally, Lu et al. developed a COF containing thiophene and benzodithiazole units (HDU-6-COF) (Figure 9g) [83]. Their mechanistic study confirmed that Cr(VI) reduction proceeds via direct electron transfer and $\cdot O_2^-$ involvement in the photocatalytic process.

Organic dyes have become significant water pollutants due to their widespread use in industries such as food processing or textiles. Table 3 presents various strategies of designing COF-based photocatalysts to remove these pollutants (Figure 10), particularly rhodamine B (RhB), methyl orange (MO), methylene blue (MB), mordant black 17 (MB17), Eriochrome black A and T (EBA and EBT), rose bengal (RB), and methyl green (MG).

Table 3. COF-based photocatalysts for degradation of organic dyes in water.

Pollutant	COF Name (Linkage Type)	Design Principle	ROS Involved	Ref.
Rhodamine B	COF-PD/AgI (imine)	COF/AgI heterojunction	$\cdot O_2^-$	[38]
	MoS_2/COF (imine)	MoS_2/COF heterojunction	$\cdot O_2^-$/·OH	[72]
	COF-HFeTBD (imine)	Donor–acceptor COFs	$^1O_2$	[85]
	HDU-105-COF (olefin)	Donor–acceptor COFs	$\cdot O_2^-$/·OH	[54]
Methylene blue	HDU-105-COF (olefin)	Donor–acceptor COFs	$\cdot O_2^-$/·OH	[54]
	C_6-TRZ-TPA COF (imine)	Donor–acceptor COFs	$\cdot O_2^-$/·OH	[86]
	TTO-COF (olefin)	Extended conjugation of COFs	$\cdot O_2^-$	[87]
Methyl orange	TTO-COF (olefin)	Extended conjugation of COFs	$\cdot O_2^-$	[87]
	COF_{A+C} (imine)	N-rich COFs	$\cdot O_2^-$/·OH	[88]
Rose bengal	C_6-TRZ-TPA COF (imine)	Donor–acceptor COFs	$\cdot O_2^-$/·OH	[86]
Mordant black 17	TpBD-COF (imine)	Pure COF	$\cdot O_2^-$/$^1O_2$/·OH	[89]
Eriochrome black T	TpBD-COF (imine)	Pure COF	$\cdot O_2^-$/$^1O_2$/·OH	[89]
	TFA-TTA-COF (imine)	Fluorinated COF	$\cdot O_2^-$/$^1O_2$	[90]
Eriochrome black A	TFA-TTA-COF (imine)	Fluorinated COF	$\cdot O_2^-$/$^1O_2$	[90]
Methyl green	CuO/COF (imine)	CuO/COF heterojunction	$\cdot O_2^-$	[91]

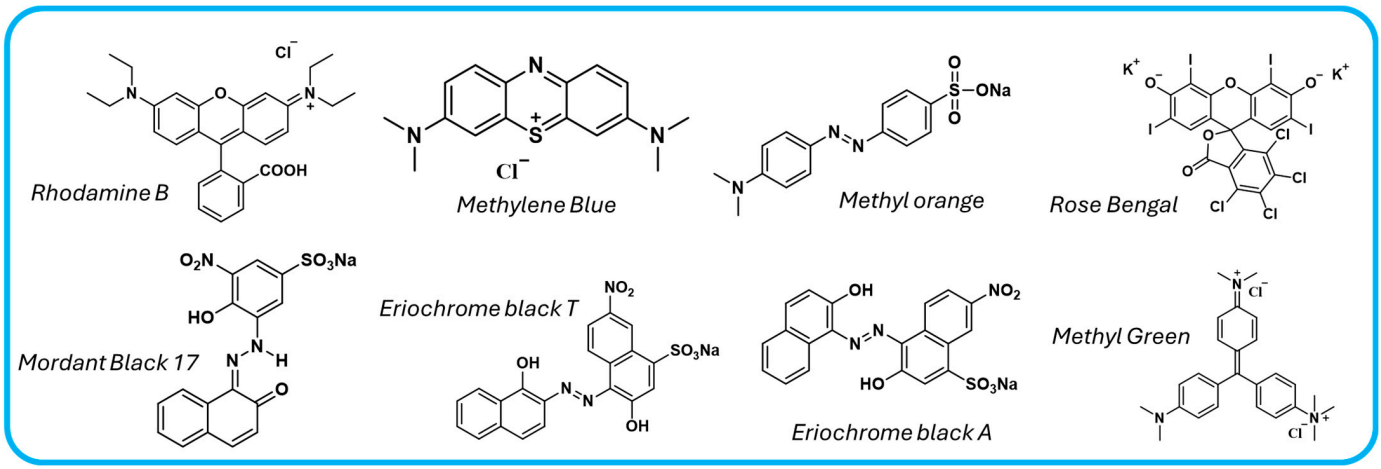


Figure 10. Chemical structures of common dyes pollutant in water.

Regarding rhodamine B, two COF-based heterojunctions (COF-PD/AgI and MoS_2/COF) previously discussed in Table 1 have also been explored for their photocatalytic degradation (Figure 11a,b) [38,72]. In both cases, $\cdot O_2^-$ is the primary reactive species responsible for degradation, while in the MoS_2/COF system, ·OH radicals also participate in the RhB photodegradation. Additionally, Liu et al. reported a D-A COF incorporating porphyrin units coordinated with Fe centers (COF-HFeTBD) (Figure 11c) [85]. Mechanistic studies reveals that the active species in this system is singlet oxygen species ($^1O_2$), generated via oxidation of $\cdot O_2$, although $\cdot O_2^-$ itself is not directly involved in the RhB oxidation.

In another approach, Wang et al. investigated a D-A olefin-linked COF (HDU-105-COF) for the photocatalytic degradation of RhB and MB (Figure 11d) [54]. Mechanistic studies indicated that both $\cdot O_2^-$ and ·OH species contribute to the process, with $\cdot O_2^-$ playing a more significant role in RhB degradation than in MB degradation. Similarly, Ruidas et al. reported a D-A imine-linked COF (C_6-TRZ-TPA COF) capable of degrading MB and RB (Figure 11e) [86]. This COF generates both $\cdot O_2^-$ and ·OH radicals, which

actively participate in the photodegradation of both dyes. Furthermore, Yang et al. designed an extended π-conjugated olefine-COF containing triazine units (TTO-COF) for the photocatalytic degradation of MB and MO (Figure 11f) [87]. In this case, the degradation of both dyes is mainly driven by the generation of $\cdot O_2^-$ radicals. Another example of MO degradation was reported by He et al., who developed an imine-linked, N-rich COF (COF_{A+C}) incorporating 4,4′,4″-(1,3,5-triazine-2,4,6-triyl) units (Figure 11g) [88]. This material generates both $\cdot O_2^-$ and ·OH radicals, which are responsible of the MO degradation (Figure 10).

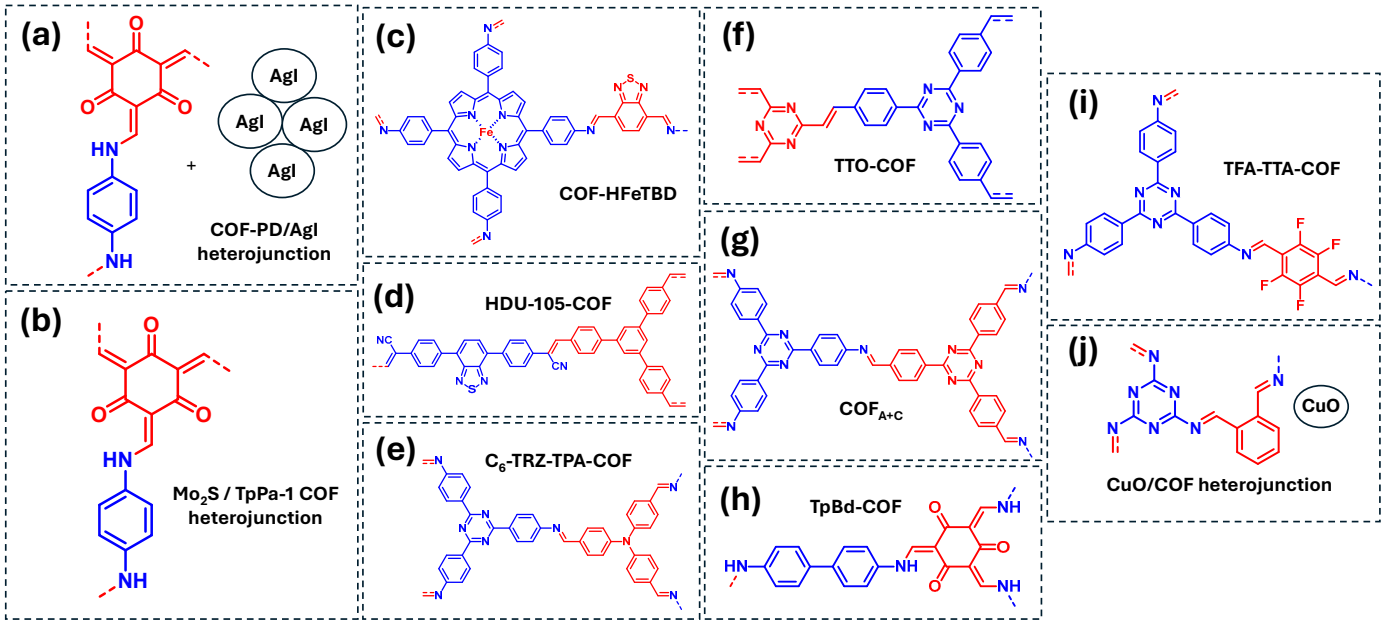


Figure 11. COF-based materials employed as photocatalysts for the degradation of dyes in water: (**a**) COF-PD/AGI heterojunction, (**b**) Mo_2S/TpPa-1 COF heterojunction, (**c**) COF-HFeTBD, (**d**) HDU-105-COF, (**e**) C_6-TRZ-TPA-COF, (**f**) TTO-COF, (**g**) COF_{A+C}, (**h**) TpBd-COF, (**i**) TFA-TTA-COF, (**j**) CuO/COF heterojunction. Red and blue coloration indicates the two building block units employed for the COF formation.

Table 3 also highlights the use of COFs as photocatalyst for the degradation of other emerging dye pollutants. For example, Xue et al. synthesized an imine-linked COF (TpBD-COF) for the photodegradation of MB17 and EBT (Figure 11h) [89]. Scavenger studies on MB17 photodegradation revealed that $\cdot O_2^-$ is the primary reactive species under visible light, while $^1O_2$ and ·OH radicals also contribute but to a lower extent. Additionally, Qi et al. developed an imine-linked, fluorinated 2D COF (TFA-TTA-COF) for the photocatalytic degradation of EBT and EBA (Figure 11i) [90]. The dominant reactive species in the degradation of both dyes is $\cdot O_2^-$, although $^1O_2$ also plays a role in the process. Finally, Wang et al. investigated the photocatalytic degradation of MG using a CuO/COF heterojunction (Figure 11j) [91]. Mechanistic studies demonstrated that $\cdot O_2^-$ is the main ROS, while direct oxidation by photogenerated holes is also favored in this heterojunction system.

Pesticides are widely used in agriculture to protect plants from pesticides; however, their persistence and toxicity make them a significant water pollutant, leading to serious environmental concerns. Table 4 presents examples of COF-based materials employed for the photocatalytic degradation of pesticides such as diazinon, parathion, imidacloprid, and pymetrozine (Figure 12).

Table 4. COF-based photocatalysts for degradation of pesticides in water.

Pollutant	COF Name (Linkage Type)	Design Principle	ROS Involved	Ref.
Diazinon and parathion	PS@COF-366 (imine)	Sulfured COF	$\cdot O_2^-$/$^1O_2$/·OH	[92]
Imidacloprid	Fe_3O_4@HMN-COF (imine)	Fe_3O_4/COF heterojunction	-	[93]
Pymetrozine	Ag_3PO_4/TpPa-1-COF (imine)	Ag_3PO_4/COF heterojunction	$\cdot O_2^-$/·OH	[94]

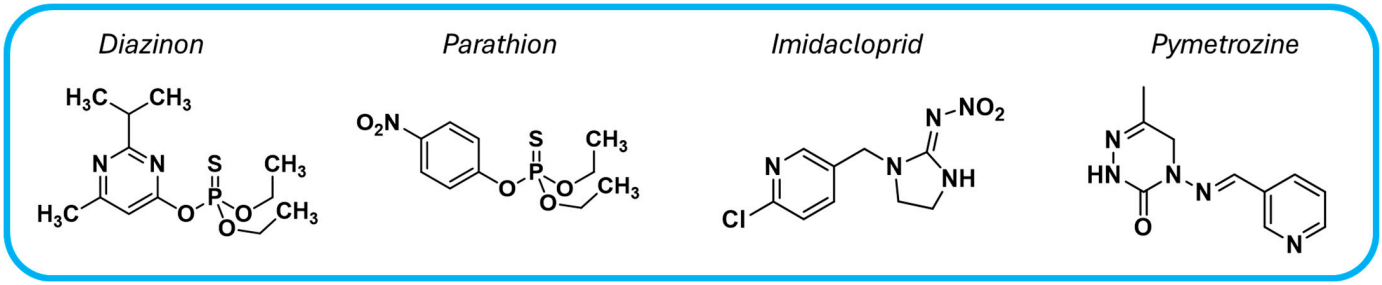


Figure 12. Chemical structures of common pesticide water pollutants.

Among them, pesticides such as diazinon and parathion have been effectively degraded using a sulfur-functionalized porphyrin-based COF, denoted as PS@COF-366 (Figure 13a) [92]. In this system, the porphyrin units act as photoantennas, facilitating photocarrier separation and enhancing photocatalytic activity. The degradation mechanism involves multiple ROS, including $\cdot O_2$, $^1O_2$, and ·OH, with $\cdot O_2^-$ playing the dominant role in the photodegradation process. Additionally, the polysulfide chains present in this COF assist in pesticide photodegradation by cleaving P-O bonds. Another example highlighted in Table 4 is the photocatalytic degradation of imidacloprid using an Fe_3O_4/COF heterojunction (Fe_3O_4@HMN-COF) (Figure 13b) [93]. This system achieved high photocatalytic efficiency (>98%) under optimized conditions. However, this study did not include a mechanistic investigation to identify the reactive species involved in the degradation process. Finally, a Ag_3PO_4/COF heterojunction (Ag_3PO_4/TpPa-1-COF) has been reported for the photocatalytic degradation of pymetrozine (Figure 13c) [94]. Mechanistic studies revealed that the degradation process proceeds via the generation of ROS, specifically $\cdot O_2^-$ and ·OH, in addition to a direct electron transfer to the substrate, further enhancing the photocatalytic performance.

Phenolic compounds are another major class of water pollutants, primarily originating from plastic industry, and pose a significant environmental threat due to their toxicity and persistence. Table 5 presents recent studies utilizing COF-based materials as photocatalysts for the degradation of these pollutants, particularly phenol, bisphenol A, and 4-chlorophenol (Figure 14).

The imine-linked, N-rich COF_{A+C} previously discussed in Table 3 and reported by He et al. was also investigated for the photodegradation of phenolic compounds (Figure 15a) [88]. Mechanistic studies suggest that the photodegradation process is mainly driven by superoxide radicals ($\cdot O_2^-$), with hydroxyl radicals (·OH) playing a supporting role. Similarly, a graphitic carbon nitride/COF heterojunction system (GCN/TD-COF) demonstrated effective phenol degradation via mechanism involving $\cdot O_2^-$ and ·OH as the main reactive species (Figure 15b) [95]. Beyond phenol degradation, different COF-based heterojunctions have been explored for the removal of bisphenol A, a widely used industrial compound of high environmental concern (Figure 14). For instance, Sun et al. reported a CdS/COF heterojunction (CdS/TFp-Azo-COF) that achieved high photocatalytic efficiency for bisphenol A degradation (Figure 15c) [39]. Mechanistic investigations identified $\cdot O_2^-$ as the dominant ROS, while ·OH played a secondary role in the photodegradation process.

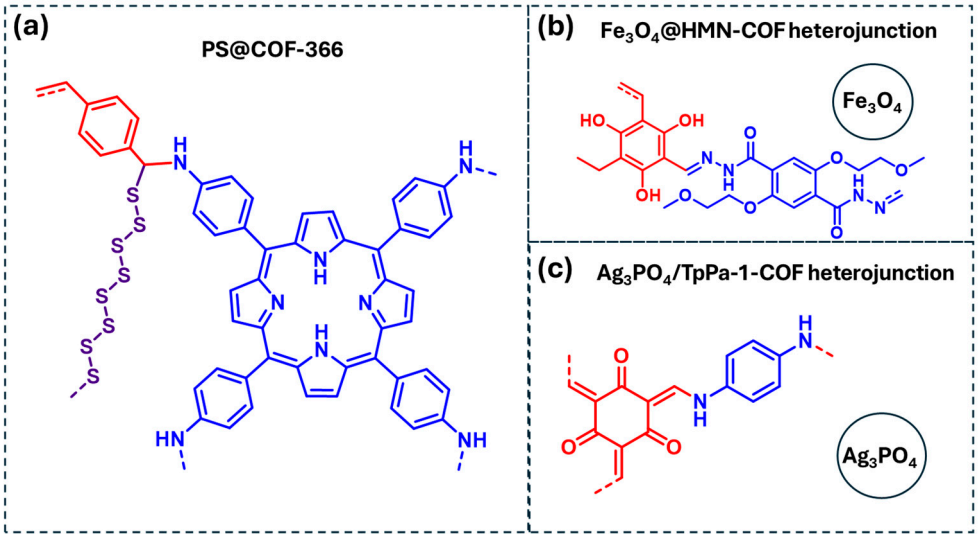


Figure 13. COF-based materials employed as photocatalysts for the degradation of pesticides in water: (**a**) PS@COF-366, (**b**) F_3O_4@HMN-COF heterojunction, (**c**) Ag_3PO_4/TpPa-1-COF heterojunction. Red and blue coloration indicates the two building block units employed for the COF formation.

Table 5. COF-based photocatalysts for degradation of phenolic compounds in water.

Pollutant	COF Name (Linkage Type)	Design Principle	ROS Involved	Ref.
Phenol	COF_{A+C} (imine)	N-rich COFs	$\cdot O_2^-$/·OH	[88]
	GCN/TD-COF (imine)	GCN/COF heterojunction	$\cdot O_2^-$/·OH	[95]
Bisphenol-A	CdS/TFp-Azo-COF (imine)	CdS/COF heterojunction	$\cdot O_2^-$/·OH	[39]
	NM-125$(Ti)_{0.4}$@TpTta-COF (imine)	MOF/COF heterojunction	$\cdot O_2^-$/$^1O_2$/·OH	[36]
	MIL-101-NH_2@COF-TpMA (imine)	MOF/COF heterojunction	·OH/$SO_4^{-\cdot}$	[63]
4-chlorophenol	Bi/TP-BDDA-COF (imine)	Bi/COF heterojunction	$\cdot O_2^-$/·OH	[96]

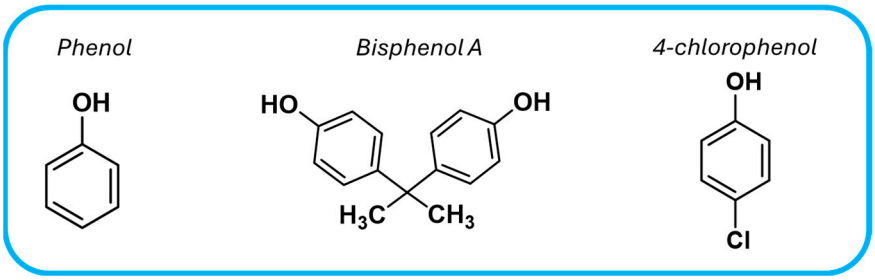


Figure 14. Chemical structures of common phenolic-compound water pollutants.

In addition, MOF/COF heterojunctions have been developed to enhance photocatalytic degradation. Yang et al. combined a Ti-based MOF with the TpTta-COF, forming the hybrid NM-125$(Ti)_{0.4}$@TpTta-COF (Figure 15d) [36]. Scavenger experiments revealed that the degradation of bisphenol A occurs through the generation of multiple ROS, including $\cdot O_2^-$, $^1O_2$, and ·OH. Lv et al. also explored a COF/MOF hybrid formed by the combination of MIL-101-NH_2 and COF-TpMA to form MIL-101-NH_2@COF-TpMA (Figure 15e) [63]. This hybrid system demonstrated that bisphenol A degradation was mainly mediated by ·OH, with SO_4^- also participating in the oxidation process. Finally, the last example of

Table 5 consists of a Bi/COF heterojunction (Bi/TP-BDDA-COF) reported as an efficient photocatalyst for the degradation of 4-chlorophenol, with $\cdot O_2^-$ and ·OH identified as the key reactive species driving the process (Figure 15f) [96].

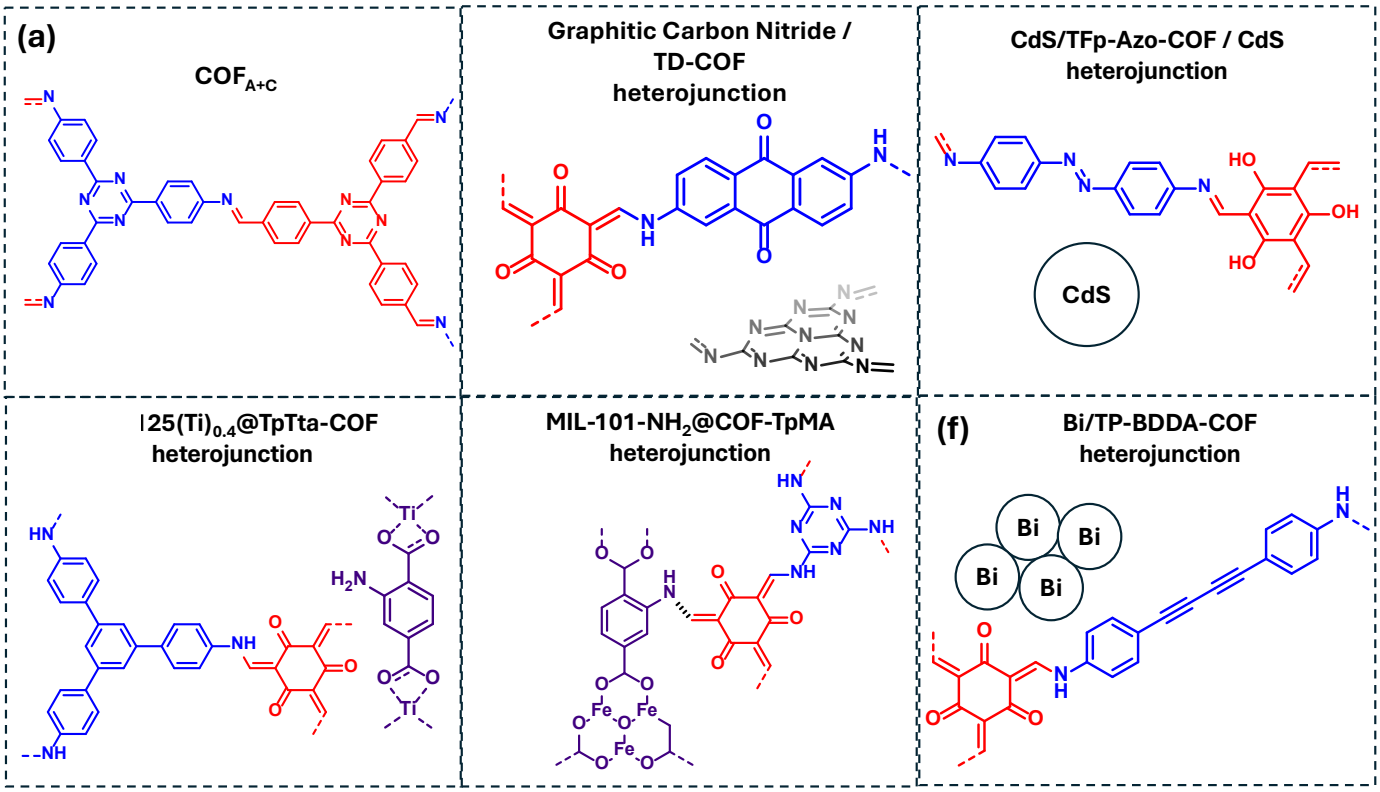


Figure 15. COF-based materials employed as photocatalysts for the degradation of phenolic compounds in water: (**a**) COF_{A+C}, (**b**) graphitic carbon nitride/TD-COF heterojunction, (**c**) CdS/TFp-Azo-COF/CdS heterojunction, (**d**) NM-125(Ti)$_{0.4}$@TpTta-COF heterojunction, (**e**) MIL-101-NH_2@COF-TpMa heterojunction, (**f**) Bi/TP-BDDA-COF heterojunction. Red and blue coloration indicates the two building block units employed for the COF formation.

5. Concluding Remarks

In general, the review of the available literature presented in this manuscript highlights the enormous potential of COFs for photocatalytic water decontamination applications. The growing plethora of available building blocks, coupled with constant improvements in synthetic processes and in the design of covalent organic structures, make these materials a valuable target for environmental applications. The stablished mechanistic landscape and the dependence of the pathways followed on the structural features of materials resulted in stabilizing several structure–reactivity relationships. In this review, we highlighted the role of extended conjugation, the presence of donor–acceptor moieties, and the strategies to modulate the optical bandgap as main tools to direct the photocatalytic activity of COFs. The state of the art makes it foreseeable that new COF-type materials with improved activities for a wide variety of pollutants will emerge. Furthermore, dual photocatalytic systems are appearing in the literature, in which one pollutant is simultaneously oxidized and another is reduced, which promise to be effective alternatives for decontaminating water with pollutants of various kinds. Despite the wide range of pollutants tackled by photocatalytic systems based on COFs, some aspects related to water decontamination remain elusive. An especially relevant challenge consists of micro/nano-plastic particles, which could be an important subject of future research.

The processes achieved by photocatalytic COFs constitute a very promising field of research of undoubted environmental interest. However, some aspects inherent to the nature of COF materials constitute major drawbacks for translating the basic research reported here into practical applications. First, water decontamination requires large-scale production of active materials, which should involve low-cost synthesis. At present, most photoactive COFs are constituted by high added-value organic building blocks. Therefore, the use of widely available organic structures, such as natural products, should be explored. In addition, COFs are often obtained as powdered samples. However, powders are difficult to incorporate into practical devices due to their difficult immobilization or inconvenient clogging phenomena. Therefore, COF processing strategies should be applied to incorporate these organic materials into parts or devices, which would involve generating structures of at least several millimeters in size.

Overall, the state of the art shown in this summary confirms that photocatalytic applications of COFs for water remediation have great growth potential. However, further progress is needed on new challenges such as the deactivation of biological pathogens, removal of microplastics, large-scale production of COFs, and their incorporation into practical devices. This review provides a starting point to encourage researchers to move towards new developments that expand the applicability of covalent organic frameworks to overcome common drawbacks of traditional water decontamination processes.

Funding: Ruben Mas-Balleste acknowledges the financial support provided by the Spanish Ministry of Science and Innovation MCIN/AEI/FEDER (10.13039/501100011033) through the project PID2022-141016OB-I00 via Proyectos de Generación de Conocimiento 2022. Alicia Moya acknowledges the Spanish Government and the Funds Next Generation of the European Union through the grant Maria Zambrano-UAM (CA3/RSUE/2021-00648). Miguel Sanchez-Fuente thanks Ministerio de Ciencia e Innovación for a FPI contract (PRE2020-092295).

Institutional Review Board Statement: Not applicable.

Data Availability Statement: No new data were created or analyzed in this study. Data sharing is not applicable to this article.

Conflicts of Interest: The authors declare no conflicts of interest.

Abbreviations

The following abbreviations are used in this manuscript:

COF	Covalent Organic Frameworks
ROS	Reactive Oxygen Species
VB	Valence Band
CB	Conduction Band
ISC	Intersystem Crossing
EIS	Electrochemical Impedance Spectroscopy
XPS	X-ray Photoelectron Spectroscopy
UPS	Ultraviolet Photoelectron Spectroscopy
D-A	Donor–Acceptor
BPA	Bisphenol A
MOFs	Metal–Organic Frameworks
Vfb	Flat Band Potential
Ef	Fermi Level
HOMO	Highest Occupied Molecular Orbital
LUMO	Lowest Unoccupied Molecular Orbital
SET	Single Electron Transfer
EnT	Energy Transfer

PC	Photocatalyst
SED	Sacrificial Electron Donor
FRET	Förster Resonance Energy Transfer
Ered	Reduction Potential
Eox	Oxidation Potential
EPR	Electron Paramagnetic Resonance
TC	Tetracycline
ACTP	Acetaminophen
SMT	Sulfamethazine
SMX	Sulfamethoxazole
RhB	Rhodamine B
MB	Methylene Blue
MO	Methyl Orange
MB17	Mordant Black 17
EBA	Eriochrome Black A
EBT	Eriochrome Black T
RB	Rose Bengal
MG	Methyl Green

References

1. World Bank Group. Water. Available online: https://www.worldbank.org/en/topic/water/overview (accessed on 22 September 2024).
2. Semrany, S.; Favier, L.; Djelal, H.; Taha, S.; Amrane, A. Bioaugmentation: Possible Solution in the Treatment of Bio-Refractory Organic Compounds (Bio-ROCs). *Biochem. Eng. J.* **2012**, *69*, 75–86. [CrossRef]
3. Samarasinghe, L.V.; Muthukumaran, S.; Baskaran, K. Recent Advances in Visible Light-Activated Photocatalysts for Degradation of Dyes: A Comprehensive Review. *Chemosphere* **2024**, *349*, 140818. [CrossRef] [PubMed]
4. Islam, M.; Kumar, S.; Saxena, N.; Nafees, A. Photocatalytic Degradation of Dyes Present in Industrial Effluents: A Review. *ChemistrySelect* **2023**, *8*, e202301048. [CrossRef]
5. Ruziwa, D.T.; Oluwalana, A.E.; Mupa, M.; Meili, L.; Selvasembian, R.; Nindi, M.M.; Sillanpaa, M.; Gwenzi, W.; Chaukura, N. Pharmaceuticals in Wastewater and Their Photocatalytic Degradation Using Nano-Enabled Photocatalysts. *J. Water Process Eng.* **2023**, *54*, 103880. [CrossRef]
6. Vaya, D.; Surolia, P.K. Semiconductor Based Photocatalytic Degradation of Pesticides: An Overview. *Environ. Technol. Innov.* **2020**, *20*, 101128. [CrossRef]
7. Shoneye, A.; Sen Chang, J.; Chong, M.N.; Tang, J. Recent Progress in Photocatalytic Degradation of Chlorinated Phenols and Reduction of Heavy Metal Ions in Water by TiO_2-Based Catalysts. *Int. Mater. Rev.* **2022**, *67*, 47–64. [CrossRef]
8. Arora, R. Adsorption of Heavy Metals—A Review. *Mater. Today Proc.* **2019**, *18*, 4745–4750. [CrossRef]
9. Okoli, B.J.; Modise, J.S. Sequestration of Pb(II) and Cr(VI) from Aqueous Environment Using Low-Cost Immobilised Tannin Resin. *SN Appl. Sci.* **2019**, *1*, 194. [CrossRef]
10. Chu, C.; Ryberg, E.C.; Loeb, S.K.; Suh, M.-J.; Kim, J.-H. Water Disinfection in Rural Areas Demands Unconventional Solar Technologies. *Acc. Chem. Res.* **2019**, *52*, 1187–1195. [CrossRef]
11. Joseph, L.; Jun, B.-M.; Flora, J.R.V.; Park, C.M.; Yoon, Y. Removal of Heavy Metals from Water Sources in the Developing World Using Low-Cost Materials: A Review. *Chemosphere* **2019**, *229*, 142–159. [CrossRef]
12. Younis, S.A.; Kim, K.-H. Heterogeneous Photocatalysis Scalability for Environmental Remediation: Opportunities and Challenges. *Catalysts* **2020**, *10*, 1109. [CrossRef]
13. Gaya, U.I.; Abdullah, A.H. Heterogeneous Photocatalytic Degradation of Organic Contaminants over Titanium Dioxide: A Review of Fundamentals, Progress and Problems. *J. Photochem. Photobiol. C Photochem. Rev.* **2008**, *9*, 1–12. [CrossRef]
14. Moya, A.; Cherevan, A.; Marchesan, S.; Gebhardt, P.; Prato, M.; Eder, D.; Vilatela, J.J. Oxygen Vacancies and Interfaces Enhancing Photocatalytic Hydrogen Production in Mesoporous CNT/TiO_2 Hybrids. *Appl. Catal. B Environ.* **2015**, *179*, 574–582. [CrossRef]
15. Bagheri, S.; TermehYousefi, A.; Do, T.-O. Photocatalytic Pathway toward Degradation of Environmental Pharmaceutical Pollutants: Structure, Kinetics and Mechanism Approach. *Catal. Sci. Technol.* **2017**, *7*, 4548–4569. [CrossRef]
16. Armaković, S.J.; Savanović, M.M.; Armaković, S. Spray-Deposited TiO_2 Layers on Aluminum Foil for Sustainable Water Remediation. *Crystals* **2024**, *14*, 875. [CrossRef]
17. Côté, A.P.; Benin, A.I.; Ockwig, N.W.; O'Keeffe, M.; Matzger, A.J.; Yaghi, O.M. Porous, Crystalline, Covalent Organic Frameworks. *Science* **2005**, *310*, 1166–1170. [CrossRef]

18. López-Magano, A.; Jiménez-Almarza, A.; Alemán, J.; Mas-Ballesté, R. Metal–Organic Frameworks (MOFs) and Covalent Organic Frameworks (COFs) Applied to Photocatalytic Organic Transformations. *Catalysts* **2020**, *10*, 720. [CrossRef]
19. López-Magano, A.; Salaverri, N.; Marzo, L.; Mas-Ballesté, R.; Alemán, J. Synergistic Combination of Triazine and Phenanthroline Moieties in a Covalent Triazine Framework Tailored for Heterogeneous Photocatalytic Metal-Free C-Br and C-Cl Activation. *Appl. Catal. B Environ.* **2022**, *317*, 121791. [CrossRef]
20. Liu, F.; Ma, Z.; Deng, Y.; Wang, M.; Zhou, P.; Liu, W.; Guo, S.; Tong, M.; Ma, D. Tunable Covalent Organic Frameworks with Different Heterocyclic Nitrogen Locations for Efficient Cr(VI) Reduction, Escherichia Coli Disinfection, and Paracetamol Degradation under Visible-Light Irradiation. *Environ. Sci. Technol.* **2021**, *55*, 5371–5381. [CrossRef]
21. Fávaro, M.A.; Yang, J.; Ditz, D.; Küçükkeçeci, H.; Alkhurisi, M.H.; Bergwinkl, S.; Thomas, A.; Quadrelli, E.A.; Palkovits, R.; Canivet, J.; et al. Pyrene- and Bipyridine-Based Covalent Triazine Framework as Versatile Platform for Photocatalytic Solar Fuels Production. *ChemCatChem* **2023**, *15*, e202300197. [CrossRef]
22. Zhao, J.; Ren, J.; Zhang, G.; Zhao, Z.; Liu, S.; Zhang, W.; Chen, L. Donor-Acceptor Type Covalent Organic Frameworks. *Chem. A Eur. J.* **2021**, *27*, 10781–10797. [CrossRef] [PubMed]
23. Wang, L.; Zhu, W. Organic Donor-Acceptor Systems for Photocatalysis. *Adv. Sci.* **2024**, *11*, 2307227. [CrossRef] [PubMed]
24. Chen, W.; Wang, L.; Mo, D.; He, F.; Wen, Z.; Wu, X.; Xu, H.; Chen, L. Modulating Benzothiadiazole-Based Covalent Organic Frameworks via Halogenation for Enhanced Photocatalytic Water Splitting. *Angew. Chem. Int. Ed.* **2020**, *59*, 16902–16909. [CrossRef]
25. Li, S.; Li, L.; Li, Y.; Dai, L.; Liu, C.; Liu, Y.; Li, J.; Lv, J.; Li, P.; Wang, B. Fully Conjugated Donor–Acceptor Covalent Organic Frameworks for Photocatalytic Oxidative Amine Coupling and Thioamide Cyclization. *ACS Catal.* **2020**, *10*, 8717–8726. [CrossRef]
26. Qin, C.; Wu, X.; Tang, L.; Chen, X.; Li, M.; Mou, Y.; Su, B.; Wang, S.; Feng, C.; Liu, J.; et al. Dual Donor-Acceptor Covalent Organic Frameworks for Hydrogen Peroxide Photosynthesis. *Nat. Commun.* **2023**, *14*, 5238. [CrossRef]
27. Chen, X.-R.; Cui, W.-R.; Liang, R.-P.; Zhang, C.-R.; Xu, R.-H.; Jiang, W.; Qiu, J.-D. Band Gap Engineering in Vinylene-Linked Covalent Organic Frameworks for Enhanced Photocatalytic Degradation of Organic Contaminants and Disinfection of Bacteria. *ACS Appl. Bio Mater.* **2021**, *4*, 6502–6511. [CrossRef]
28. Deng, M.; Wang, L.; Wen, Z.; Chakraborty, J.; Sun, J.; Wang, G.; Van Der Voort, P. Donor–Acceptor Sp2 Covalent Organic Frameworks for Photocatalytic H_2O_2 Production and Tandem Bisphenol-A Degradation. *Green Chem.* **2024**, *26*, 3239–3248. [CrossRef]
29. Lin, Q.; Yusran, Y.; Xing, J.; Li, Y.; Zhang, J.; Su, T.; Yang, L.; Suo, J.; Zhang, L.; Li, Q.; et al. Structural Conjugation Tuning in Covalent Organic Frameworks Boosts Charge Transfer and Photocatalysis Performances. *ACS Appl. Mater. Interfaces* **2024**, *16*, 5869–5880. [CrossRef]
30. Deng, M.; Sun, J.; Laemont, A.; Liu, C.; Wang, L.; Bourda, L.; Chakraborty, J.; Van Hecke, K.; Morent, R.; De Geyter, N.; et al. Extending the π-Conjugation System of Covalent Organic Frameworks for More Efficient Photocatalytic H_2O_2 Production. *Green Chem.* **2023**, *25*, 3069–3076. [CrossRef]
31. Chen, Z.; Wang, J.; Hao, M.; Xie, Y.; Liu, X.; Yang, H.; Waterhouse, G.I.N.; Wang, X.; Ma, S. Tuning Excited State Electronic Structure and Charge Transport in Covalent Organic Frameworks for Enhanced Photocatalytic Performance. *Nat. Commun.* **2023**, *14*, 1106. [CrossRef]
32. Cai, Y.; Ling, Q.; Yi, Y.; Chen, Z.; Yang, H.; Hu, B.; Liang, L.; Wang, X. Application of Covalent Organic Frameworks in Environmental Pollution Management. *Appl. Catal. A Gen.* **2022**, *643*, 118733. [CrossRef]
33. Krishna, D.N.G.; Philip, J. Review on Surface-Characterization Applications of X-Ray Photoelectron Spectroscopy (XPS): Recent Developments and Challenges. *Appl. Surf. Sci. Adv.* **2022**, *12*, 100332. [CrossRef]
34. Whitten, J.E. Ultraviolet Photoelectron Spectroscopy: Practical Aspects and Best Practices. *Appl. Surf. Sci. Adv.* **2023**, *13*, 100384. [CrossRef]
35. He, R.; Xue, K.; Wang, J.; Yang, T.; Sun, R.; Wang, L.; Yu, X.; Omeoga, U.; Wang, W.; Yang, T.; et al. Design and Synthesis of La^{3+}-, Sb^{3+}-Doped MOF-In2S3@FcDc-TAPT COFs Hybrid Materials with Enhanced Photocatalytic Activity. *J. Mater. Sci.* **2019**, *54*, 14690–14706. [CrossRef]
36. Yang, L.; Wang, Y.; Yuan, J.; Wang, G.; Cao, Q.; Fei, H.; Li, M.; Shao, J.; Li, H.; Lu, J. Construction of Covalent-Integrated MOFs@COFs Composite Material for Efficient Synergistic Adsorption and Degradation of Pollutants. *Chem. Eng. J.* **2022**, *446*, 137095. [CrossRef]
37. Zhang, Y.; Hu, Y.; Zhao, J.; Park, E.; Jin, Y.; Liu, Q.; Zhang, W. Covalent Organic Framework-Supported Fe–TiO2 Nanoparticles as Ambient-Light-Active Photocatalysts. *J. Mater. Chem. A* **2019**, *7*, 16364–16371. [CrossRef]
38. Liu, F.; Nie, C.; Dong, Q.; Ma, Z.; Liu, W.; Tong, M. AgI Modified Covalent Organic Frameworks for Effective Bacterial Disinfection and Organic Pollutant Degradation under Visible Light Irradiation. *J. Hazard. Mater.* **2020**, *398*, 122865. [CrossRef]
39. Sun, C.; Karuppasamy, L.; Gurusamy, L.; Yang, H.-J.; Liu, C.-H.; Dong, J.; Wu, J.J. Facile Sonochemical Synthesis of CdS/COF Heterostructured Nanocomposites and Their Enhanced Photocatalytic Degradation of Bisphenol-A. *Sep. Purif. Technol.* **2021**, *271*, 118873. [CrossRef]

40. Liu, J.; Ren, X.; Li, C.; Wang, M.; Li, H.; Yang, Q. Assembly of COFs Layer and Electron Mediator on Silica for Visible Light Driven Photocatalytic NADH Regeneration. *Appl. Catal. B Environ.* **2022**, *310*, 121314. [CrossRef]
41. Yao, Y.; Hu, Y.; Hu, H.; Chen, L.; Yu, M.; Gao, M.; Wang, S. Metal-Free Catalysts of Graphitic Carbon Nitride–Covalent Organic Frameworks for Efficient Pollutant Destruction in Water. *J. Colloid Interface Sci.* **2019**, *554*, 376–387. [CrossRef]
42. Xu, J.; Yang, C.; Bi, S.; Wang, W.; He, Y.; Wu, D.; Liang, Q.; Wang, X.; Zhang, F. Vinylene-Linked Covalent Organic Frameworks (COFs) with Symmetry-Tuned Polarity and Photocatalytic Activity. *Angew. Chem. Int. Ed.* **2020**, *59*, 23845–23853. [CrossRef] [PubMed]
43. Wang, L.; Lian, R.; Zhang, Y.; Ma, X.; Huang, J.; She, H.; Liu, C.; Wang, Q. Rational Preparation of Cocoon-like g-C3N4/COF Hybrids: Accelerated Intramolecular Charge Delivery for Photocatalytic Hydrogen Evolution. *Appl. Catal. B Environ.* **2022**, *315*, 121568. [CrossRef]
44. Nagar, A.; Singh, G.; Alam, A.; Pachfule, P.; Nagaraja, C.M. Design of Donor–Acceptor Covalent Organic Frameworks for Photocatalytic Hydrogen Generation. *Mater. Chem. Front.* **2025**, *9*, 1421–1430. [CrossRef]
45. Li, Z.; Deng, T.; Ma, S.; Zhang, Z.; Wu, G.; Wang, J.; Li, Q.; Xia, H.; Yang, S.-W.; Liu, X. Three-Component Donor−π–Acceptor Covalent–Organic Frameworks for Boosting Photocatalytic Hydrogen Evolution. *J. Am. Chem. Soc.* **2023**, *145*, 8364–8374. [CrossRef]
46. Zhong, X.; Meng, F.; Dong, Y.; Zhao, J.; Zhang, H.; Du, Y. S-Scheme Heterojunction between Donor-Acceptor Linear Polymer and g-C3N4 via Strengthened Internal Electric Field for Enhanced Photocatalytic Activity. *Mater. Today Energy* **2025**, *48*, 101773. [CrossRef]
47. Wang, J.; Yin, D.; Guo, X.; Luo, Z.; Tao, L.; Ren, J.; Zhang, Y. Fabrication of a Covalent Organic Framework-Based Heterojunction via Coupling with ZnAgInS Nanosphere with High Photocatalytic Activity. *Langmuir* **2022**, *38*, 4680–4691. [CrossRef] [PubMed]
48. Mohamadpour, F.; Amani, A.M. Photocatalytic Systems: Reactions, Mechanism, and Applications. *RSC Adv.* **2024**, *14*, 20609–20645. [CrossRef]
49. Kandoth, N.; Pérez Hernández, J.; Palomares, E.; Lloret-Fillol, J. Mechanisms of Photoredox Catalysts: The Role of Optical Spectroscopy. *Sustain. Energy Fuels* **2021**, *5*, 638–665. [CrossRef]
50. Zhou, Q.-Q.; Zou, Y.-Q.; Lu, L.-Q.; Xiao, W.-J. Visible-Light-Induced Organic Photochemical Reactions through Energy-Transfer Pathways. *Angew. Chem. Int. Ed.* **2019**, *58*, 1586–1604. [CrossRef]
51. Romero, N.A.; Nicewicz, D.A. Organic Photoredox Catalysis. *Chem. Rev.* **2016**, *116*, 10075–10166. [CrossRef]
52. Andrés, C.M.C.; de la Lastra, P.; Manuel, J.; Andrés Juan, C.; Plou, F.J.; Pérez-Lebeña, E. Superoxide Anion Chemistry—Its Role at the Core of the Innate Immunity. *Int. J. Mol. Sci.* **2023**, *24*, 1841. [CrossRef]
53. Song, J.; Lei, H.; Zhai, Y.; Dou, Z.; Ding, Y.; Han, X.; Cui, F.; Tian, Y.; Zhu, G. Exclusive Generation of a Superoxide Radical by a Porous Aromatic Framework for Fast Photocatalytic Decontamination of Mustard Gas Simulant in Room Air. *Chem. Sci.* **2024**, *15*, 15717–15724. [CrossRef]
54. Wang, C.; Lu, W.; Song, W.; Zhang, Z.; Xie, C.; Ji, Z.; Li, Y.; Wang, J. Dual Application of a Cyano-Containing Covalent Organic Framework: Photocatalytic Degradation of Dyes with Fluorescence Detection Studies. *Appl. Catal. A Gen.* **2023**, *666*, 119433. [CrossRef]
55. Xie, J.; Pan, X.; Jiang, C.; Zhao, L.; Gong, X.; Liu, Y. Enhanced Conversion of Superoxide Radical to Singlet Oxygen in Peroxymonosulfate Activation by Metal-Organic Frameworks Derived Heteroatoms Dual-Doped Porous Carbon Catalyst. *Environ. Res.* **2023**, *236*, 116745. [CrossRef]
56. Shi, T.; Wang, H.; Li, L.; Zhao, Z.; Wang, C.; Zhang, X.; Xie, Y. Enhanced Photostability in Protonated Covalent Organic Frameworks for Singlet Oxygen Generation. *Matter* **2022**, *5*, 1004–1015. [CrossRef]
57. Zhang, J.; Nosaka, Y. Mechanism of the OH Radical Generation in Photocatalysis with TiO_2 of Different Crystalline Types. *J. Phys. Chem. C* **2014**, *118*, 10824–10832. [CrossRef]
58. Nosaka, Y.; Komori, S.; Yawata, K.; Hirakawa, T.; Nosaka, A.Y. Photocatalytic ˙OH Radical Formation in TiO_2 Aqueous Suspension Studied by Several Detection Methods. *Phys. Chem. Chem. Phys.* **2003**, *5*, 4731–4735. [CrossRef]
59. Nosaka, Y.; Nosaka, A. Understanding Hydroxyl Radical (•OH) Generation Processes in Photocatalysis. *ACS Energy Lett.* **2016**, *1*, 356–359. [CrossRef]
60. Jiang, D. Covalent Organic Frameworks: An Amazing Chemistry Platform for Designing Polymers. *Chem* **2020**, *6*, 2461–2483. [CrossRef]
61. Lin, C.; Shan, Z.; Dong, C.; Lu, Y.; Meng, W.; Zhang, G.; Cai, B.; Su, G.; Park, J.H.; Zhang, K. Covalent Organic Frameworks Bearing Ni Active Sites for Free Radical-Mediated Photoelectrochemical Organic Transformations. *Sci. Adv.* **2023**, *9*, eadi9442. [CrossRef]
62. Hasija, V.; Raizada, P.; Thakur, V.K.; Ahamad, T.; Alshehri, S.M.; Thakur, S.; Nguyen, V.-H.; Van Le, Q.; Singh, P. An Overview on Photocatalytic Sulfate Radical Formation via Doped Graphitic Carbon Nitride for Water Remediation. *Curr. Opin. Chem. Eng.* **2022**, *37*, 100841. [CrossRef]

63. Lv, S.-W.; Liu, J.-M.; Li, C.-Y.; Zhao, N.; Wang, Z.-H.; Wang, S. Two Novel MOFs@COFs Hybrid-Based Photocatalytic Platforms Coupling with Sulfate Radical-Involved Advanced Oxidation Processes for Enhanced Degradation of Bisphenol A. *Chemosphere* **2020**, *243*, 125378. [CrossRef]
64. Gong, Y.; Zhao, X.; Zhang, H.; Yang, B.; Xiao, K.; Guo, T.; Zhang, J.; Shao, H.; Wang, Y.; Yu, G. MOF-Derived Nitrogen Doped Carbon Modified g-C3N4 Heterostructure Composite with Enhanced Photocatalytic Activity for Bisphenol A Degradation with Peroxymonosulfate under Visible Light Irradiation. *Appl. Catal. B Environ.* **2018**, *233*, 35–45. [CrossRef]
65. Li, X.; Guo, W.; Liu, Z.; Wang, R.; Liu, H. Fe-Based MOFs for Efficient Adsorption and Degradation of Acid Orange 7 in Aqueous Solution via Persulfate Activation. *Appl. Surf. Sci.* **2016**, *369*, 130–136. [CrossRef]
66. Sánchez-Fuente, M.; Jimenez-Almarza, A.; Alemán, J.; Mas-Ballesté, R. Solvent-Free Visible Light Photocatalytic Oxidation Processes Mediated by Transparent Films of an Imine-Based Organic Polymer. *Catalysts* **2021**, *11*, 1426. [CrossRef]
67. Luo, J.; Lu, J.; Zhang, J. Carbazole–Triazine Based Donor–Acceptor Porous Organic Frameworks for Efficient Visible-Light Photocatalytic Aerobic Oxidation Reactions. *J. Mater. Chem. A* **2018**, *6*, 15154–15161. [CrossRef]
68. Zhi, Y.; Li, K.; Xia, H.; Xue, M.; Mu, Y.; Liu, X. Robust Porous Organic Polymers as Efficient Heterogeneous Organo-Photocatalysts for Aerobic Oxidation Reactions. *J. Mater. Chem. A* **2017**, *5*, 8697–8704. [CrossRef]
69. Qian, Y.; Li, D.; Han, Y.; Jiang, H.-L. Photocatalytic Molecular Oxygen Activation by Regulating Excitonic Effects in Covalent Organic Frameworks. *J. Am. Chem. Soc.* **2020**, *142*, 20763–20771. [CrossRef]
70. Zhang, H.; Zhang, L.; Dong, S.; Duan, X.; Zhu, D.; Ni, B.-J.; Lyu, C. Regulating Energy Band Structures of Triazine Covalent Organic Frameworks with Electron-Donating/Withdrawing Substituents for Visible-Light-Responsive Photocatalytic Tetracycline Degradation and Cr(VI) Reduction. *J. Hazard. Mater.* **2023**, *446*, 130756. [CrossRef]
71. Hu, Z.; Luo, Y.; Wang, L.; Wang, Y.; Wang, Q.; Jiang, G.; Zhang, Q.; Cui, F. Synthesis of Pyrene-Based Covalent Organic Frameworks for Photocatalytic Tetracycline Degradation. *ACS Appl. Polym. Mater.* **2023**, *5*, 9263–9273. [CrossRef]
72. Khaing, K.K.; Yin, D.; Ouyang, Y.; Xiao, S.; Liu, B.; Deng, L.; Li, L.; Guo, X.; Wang, J.; Liu, J.; et al. Fabrication of 2D–2D Heterojunction Catalyst with Covalent Organic Framework (COF) and MoS2 for Highly Efficient Photocatalytic Degradation of Organic Pollutants. *Inorg. Chem.* **2020**, *59*, 6942–6952. [CrossRef] [PubMed]
73. Hou, Y.; Liu, F.; Zhang, B.; Tong, M. Thiadiazole-Based Covalent Organic Frameworks with a Donor–Acceptor Structure: Modulating Intermolecular Charge Transfer for Efficient Photocatalytic Degradation of Typical Emerging Contaminants. *Environ. Sci. Technol.* **2022**, *56*, 16303–16314. [CrossRef] [PubMed]
74. Ge, S.; Cai, Y.; Deng, L.; Jin, M.; Qu, X.; Liu, H.; Wang, H.; Wang, B. Constructing Heptazine-COF@TiO_2 Heterojunction Photocatalysts for Efficient Photodegradation of Acetaminophen under Visible Light. *ChemPlusChem* **2024**, *89*, e202400139. [CrossRef]
75. Ben, H.; Yan, G.; Liu, H.; Ling, C.; Fan, Y.; Zhang, X. Local Spatial Polarization Induced Efficient Charge Separation of Squaraine-Linked COF for Enhanced Photocatalytic Performance. *Adv. Funct. Mater.* **2022**, *32*, 2104519. [CrossRef]
76. Qi, L.; Xiao, C.; Lu, W.; Zhang, H.; Zhou, Y.; Qi, J.; Yang, Y.; Zhu, Z.; Li, J. Triazine-Based Covalent Organic Framework/ g-C3N4 Heterojunction toward Highly Efficient Photoactivation of Peroxydisulfate for Sulfonamides Degradation. *Sep. Purif. Technol.* **2025**, *354*, 128758. [CrossRef]
77. Dong, Z.; Zhang, L.; Gong, J.; Zhao, Q. Covalent Organic Framework Nanorods Bearing Single Cu Sites for Efficient Photocatalysis. *Chem. Eng. J.* **2021**, *403*, 126383. [CrossRef]
78. Zhong, X.; Ling, Q.; Ren, Z.; Hu, B. Immobilization of U(VI) onto Covalent Organic Frameworks with the Different Periodic Structure by Photocatalytic Reduction. *Appl. Catal. B Environ.* **2023**, *326*, 122398. [CrossRef]
79. Ling, Q.; Kuang, P.; Zhong, X.; Hu, B. 2D Redox-Active COF with the Anthraquinone Structure for Photocatalytic Reduction of Uranium. *Appl. Surf. Sci.* **2023**, *639*, 158220. [CrossRef]
80. Huang, Q.; Zhang, H.; Yang, H.; Yu, Z.; Xu, Z.; Li, Z.; Gao, Z.; Zou, J.-P. Site Engineering of Covalent Organic Frameworks to Increase Charge Transfer Channels and Provide Hydrogen Bond toward Enhanced Photocatalytic Reduction of U(VI). *Appl. Catal. B Environ. Energy* **2025**, *362*, 124721. [CrossRef]
81. Hao, M.; Chen, Z.; Liu, X.; Liu, X.; Zhang, J.; Yang, H.; Waterhouse, G.I.N.; Wang, X.; Ma, S. Converging Cooperative Functions into the Nanospace of Covalent Organic Frameworks for Efficient Uranium Extraction from Seawater. *CCS Chem.* **2022**, *4*, 2294–2307. [CrossRef]
82. Chen, W.; Yang, Z.; Xie, Z.; Li, Y.; Yu, X.; Lu, F.; Chen, L. Benzothiadiazole Functionalized D–A Type Covalent Organic Frameworks for Effective Photocatalytic Reduction of Aqueous Chromium(VI). *J. Mater. Chem. A* **2019**, *7*, 998–1004. [CrossRef]
83. Lu, W.; Wang, C.; Bai, Y.; Xie, C.; Zhang, Z.; Song, W.; Wang, J. A Novel Covalent Organic Framework for Efficient Photocatalytic Reduction of Cr(VI) and Synergistic Removal of Organic Pollutants under Visible Light Irradiation. *Environ. Sci. Nano* **2024**, *11*, 229–240. [CrossRef]
84. Cao, D.; Guan, J.; Du, J.; Sun, Q.; Ma, J.; Li, J.; Liu, J.; Sheng, G. Halogen-Functionalized Covalent Organic Frameworks for Photocatalytic Cr(VI) Reduction under Visible Light. *J. Hazard. Mater.* **2024**, *476*, 134956. [CrossRef]

85. Liu, C.; Chen, M.; Li, H.; Shi, Q.; Feng, Y.; Zhang, B. Crystalline Covalent Organic Frameworks Based on Mixed Metallo- and Tetrahydroporphyrin Monomers for Use as Efficient Photocatalysts in Dye Pollutant Removal. *Cryst. Growth Des.* **2022**, *22*, 4745–4756. [CrossRef]
86. Ruidas, S.; Chowdhury, A.; Ghosh, A.; Ghosh, A.; Mondal, S.; Wonanke, A.D.D.; Addicoat, M.; Das, A.K.; Modak, A.; Bhaumik, A. Covalent Organic Framework as a Metal-Free Photocatalyst for Dye Degradation and Radioactive Iodine Adsorption. *Langmuir* **2023**, *39*, 4071–4081. [CrossRef]
87. Yang, Y.; Niu, H.; Xu, L.; Zhang, H.; Cai, Y. Triazine Functionalized Fully Conjugated Covalent Organic Framework for Efficient Photocatalysis. *Appl. Catal. B Environ.* **2020**, *269*, 118799. [CrossRef]
88. He, S.; Yin, B.; Niu, H.; Cai, Y. Targeted Synthesis of Visible-Light-Driven Covalent Organic Framework Photocatalyst via Molecular Design and Precise Construction. *Appl. Catal. B Environ.* **2018**, *239*, 147–153. [CrossRef]
89. Xue, H.; Xiong, S.; Mi, K.; Wang, Y. Visible-Light Degradation of Azo Dyes by Imine-Linked Covalent Organic Frameworks. *Green Energy Environ.* **2023**, *8*, 194–199. [CrossRef]
90. Qi, W.; Wu, Q.; Wang, W.; Feng, J.; Su, Q. Fluorinated Covalent Organic Framework Materials for Photocatalytically Driven Benzylamine Coupling and Azo Dyes Degradation. *J. Photochem. Photobiol. A Chem.* **2023**, *437*, 114502. [CrossRef]
91. Wang, A.; Chen, X.; Tang, H.; Huang, F.; Yao, D. Removal of Methyl Green by CuO/COF Photocatalysts with Enhanced Adsorption and Photocatalytic Activity. *ChemistrySelect* **2024**, *9*, e202404454. [CrossRef]
92. Karimi, D.; Khajeh, M.; Oveisi, A.R.; Bohlooli, M.; Khatibi, A.; Neyband, R.S.; Luque, R. Sulfur-Functionalized Porphyrin-Based Covalent Organic Framework as a Metal-Free Dual-Functional Catalyst for Photodegradation of Organophosphorus Pesticides under Visible-LED-Light. *Environ. Pollut.* **2023**, *334*, 122109. [CrossRef] [PubMed]
93. AlNeyadi, S.S.; Alhassani, M.T.; Mukhtar, M.R.; Alblooshi, H.K.; Jama, S.A.; Al Mujaini, I.; Aleissaee, A.S. Hydrophilic Magnetic COFs: The Answer to Photocatalytic Degradation and Removal of Imidacloprid Insecticide. *Heliyon* **2024**, *10*, e39042. [CrossRef]
94. Liu, J.; Feng, C.; Li, Y.; Zhang, Y.; Liang, Q.; Xu, S.; Li, Z.; Wang, S. Photocatalytic Detoxification of Hazardous Pymetrozine Pesticide over Two-Dimensional Covalent-Organic Frameworks Coupling with Ag_3PO_4 Nanospheres. *Sep. Purif. Technol.* **2022**, *288*, 120644. [CrossRef]
95. Hu, H.; Hu, Y.; Kong, W.; Tao, Y.; Jiang, Q.; Wang, J.; Li, C.; Xie, H.; Shi, Y.; Li, Y.; et al. The Photocatalytic Mineralization of Phenolic Wastewater via Self-Generation and -Activation of H_2O_2 Technology. *J. Environ. Chem. Eng.* **2023**, *11*, 111108. [CrossRef]
96. Ma, S.-H.; Jin, W.-L.; Li, W.; Wang, H.-Y.; Zhu, L.-N.; Zeng, M.; Kong, D.-M. Plasmonic Bi/COF Nanoheterojunctions for Visible-Light Photodegradation of Phenolic Pollutants. *ACS Appl. Nano Mater.* **2023**, *6*, 14151–14164. [CrossRef]

Disclaimer/Publisher's Note: The statements, opinions and data contained in all publications are solely those of the individual author(s) and contributor(s) and not of MDPI and/or the editor(s). MDPI and/or the editor(s) disclaim responsibility for any injury to people or property resulting from any ideas, methods, instructions or products referred to in the content.